Behaviour of Fibre Reinforced Polymer (FRP) Stirrups as Shear Reinforcement for Concrete Structures

by

Ryan David Morphy

A Thesis
Presented to the Faculty of Graduate Studies
in Partial Fulfillment of the Requirements
for the Degree of

Master of Science

Structural Engineering Division
Department of Civil and Geological Engineering
University of Manitoba
Winnipeg, Manitoba

THE UNIVERSITY OF MANITOBA

FACULTY OF GRADUATE STUDIES

*****

COPYRIGHT PERMISSION PAGE

Behaviour of Fibre Reinforced Polymer (FRP) Stirrups as Shear Reinforcement for Concrete Structures

BY

Ryan David Morphy

A Thesis/Practicum submitted to the Faculty of Graduate Studies of The University of Manitoba in partial fulfillment of the requirements of the degree

of

Master of Science

ACKNOWLEDGMENTS

I would like to thank Dr. Sami Rizkalla for his enthusiasm for research and for his patient guidance and encouragement through the experimental phase and the eventual completion of this thesis. The knowledge, experience, and helping hand of Dr. Emile Shehata also deserves a special thank you.

The help of all of the staff and students of the R.W. McQuade Structures Laboratory at the University of Manitoba throughout the construction and testing phases was greatly appreciated and they all deserve a sincere thanks.

This thesis would not have been possible were it not for the support provided by the Canadian Network of Centres of Excellence on Intelligent Sensing for Innovative Structures (ISIS Canada). This assistance is gratefully acknowledged.

Finally, the unwavering support, encouragement, and assistance of my wife Ewa Morphy, my parents Dave and Joan Morphy, and my brother Kyle has not gone unnoticed and unappreciated. To you and to all friends and family who have lent a helping hand or passed on an encouraging word, this thesis is dedicated.

ABSTRACT

The corrosion of steel reinforcement in reinforced concrete structures has lead to widespread deterioration of many buildings and bridges that are now in need of costly repairs. Due to their location as the outermost layer of reinforcement within a concrete structure, steel stirrups are the first to corrode. Fibre reinforced polymers (FRP) provide an alternative that does not corrode and has many other benefits such as a high strength-to-weight ratio. However, the inherent disadvantages of FRP in certain loading situations are apparent with FRP stirrups and must be accounted for in design. Loading transversely to the fibres can cause significant losses in stirrup capacity. By bending the FRP to form an end anchorage for the stirrup within the concrete, the bent portion of the bar is subjected to stresses perpendicular to the direction of the fibres and will experience strength losses. Due to the diagonal nature of shear cracks, the vertical stirrups are subjected to stresses perpendicular to the fibre direction as the crack widens. This again leads to potential strength losses.

This thesis presents the experimental program and results of 113 panel specimen tests completed to determine the losses of stirrup capacity as related to the bend effect and the inclined crack effect, determined through multiple variables. These results are analyzed to examine the effect of each variable on the strength of the stirrups. Based on these results, recommendations are made and design guidelines are presented for the use of FRP as shear reinforcement.

TABLE OF CONTENTS

CHAPTER 3: EXPERIMENTAL PROGRAM

CHAPTER 4: EXPERIMENTAL RESULTS AND DISCUSSION

CHAPTER 5: SUMMARY AND CONCLUSIONS

List of Tables

LIST OF FIGURES

CHAPTER 1: INTRODUCTION

1.1 General

Advanced composite materials in the form of Fibre Reinforced Polymers, FRP, are extensively used in the automobile industry, aerospace industry, defence, and recently in a variety of ways in civil engineering structures. Many concrete structures are deteriorating due to corrosion of the steel reinforcement, and advanced composite materials are quickly gaining popularity for use in the construction of new structures and the repair and strengthening of existing structures.

Structural engineers have a special interest in using Fibre Reinforced Polymers for reinforcing structures due to their many favourable characteristics. In comparison to steel, FRPs exhibit high tensile strength, do not corrode, are electromagnetically neutral, possess a high strength-to-weight ratio, high impact resistance and are lightweight. Fibre Reinforced Polymers provide a viable alternative to traditional steel reinforcement in concrete structures.

1.2 Research Significance

Stirrups used for shear reinforcement in concrete structural members are normally located closer to the surface of the concrete than flexural reinforcement. Due to the minimum

concrete cover provided, the stirrups therefore are more susceptible to severe environmental effects. In some cases, stirrups are exposed above the top surface of the beam to provide composite action with the slab, cast at a later stage. During this period, corrosion could be severe. FRPs have recently been introduced as reinforcement to overcome the problems related to the corrosion of steel reinforcement and the consequent deterioration of concrete structures. The research into the use of FRP as longitudinal reinforcement to date is much more extensive than for FRP as shear reinforcement. FRP for shear reinforcement has not yet been fully explored and the current available data and knowledge of behaviour is not sufficient to provide general design recommendations and guidelines to engineers.

Due to the diagonal orientation of shear cracks, the induced tensile forces are typically oriented at an angle with respect to the stirrups. Consequently, the tensile strength of the stirrups in the direction of the fibres cannot be fully developed (Maruyama et al., 1989). Bending of FRP bars into stirrups to develop sufficient anchorage could also lead to a significant reduction of the capacity (Maruyama et al., 1993; Miyata et al., 1989; Currier et al., 1994; Ehsani et al. 1995).

1.3 Objectives and Scope

The main objective of this thesis is to provide design guidelines for the use of FRP as stirrups for the shear reinforcement of concrete structures. To accomplish this, an

experimental program was undertaken to evaluate the effect of bending of the FRP bars and the orientation of shear cracks at an angle to the direction of the fibres.

In this program, single stirrup specimens were designed to simulate the behaviour mechanism of stirrups in concrete beams. The first of two phases in the experimental program examines the effect of the bend on the strength of the stirrups. In this phase the parameters include the type of material, bar diameter, stirrup anchorage, bend radius, tail length and embedment length. The second phase of the experimental program investigates the effect of the crack orientation with respect to the stirrup fibre direction. The parameters for this phase are the material type and the angle between the stirrup direction and an initiated crack. In both phases the results and behaviour of FRP stirrups are compared to steel stirrups typically used as shear reinforcement.

Chapter 2 presents the literature on FRP material and the research work on problems with the use of FRP as shear reinforcement. Chapter 3 describes the experimental program by including descriptions of the specimens and test methodology. Chapter 4 includes analysis and discussion of the results of the two-phase experimental program. Conclusions and recommendations from the research program are summarized in Chapter 5.

CHAPTER 2: LITERATURE REVIEW

2.1 General FRP Characteristics

2.1.1 FRP Definition

Fibre reinforced polymers (FRP) are composite materials that consist of load-carrying fibres encased in a resin matrix. Fibres occupy the largest volume fraction in composite laminates and are responsible for carrying the load acting on the composite (Mallick, 1993). The correct selection of fibre volumes, type, and orientation of the fibres influences the specific gravity, tensile strength, modulus of elasticity, compression strength, fatigue strength, failure mechanisms, electrical and thermal conductivity, and certainly the cost of the composite product.

There are three main types of fibres used in FRP material. These include aramid, glass, and carbon fibres. The characteristics of these fibres are shown in Figure 2-1 based on the representative values given in Table 2-1. In general, all the fibres exhibit a linear behaviour in tension up to fracture in contrast to steel with its clearly defined yield. Most fibres are characterised by a high elastic modulus, low creep and relaxation, stability at normal ambient temperatures and high tensile strength. The fibres are continuous and the diameter is in the range of 4 to 10 micrometers (Mufti et al., 1991). Individual fibres are then bundled together creating a stronger overall composite (Dolan et al., 1993).

Table 2-1 Material properties of various FRP fibres

Material	Density (kg/m3)	E (GPa)	σ_t (GPa)	ϵ_t (%)	α $10^{-6}/^{o}C$
E-glass (GFRP)	2500	70	1.5 – 2.5	1.8 – 3.0	5.0
S-glass (GFRP)	2500	86	4.8	--	--
High-Modulus Carbon (CFRP)	1950	380	2.0	0.5	-0.6 – -1.3
High-Strength Carbon (CFRP)	1720	240	2.8	1.0	-0.2 – -0.6
Carbon (CFRP)	1400	190	1.7	--	--
Kevlar 49 (AFRP)	1450	60 – 130	2.9	--	--

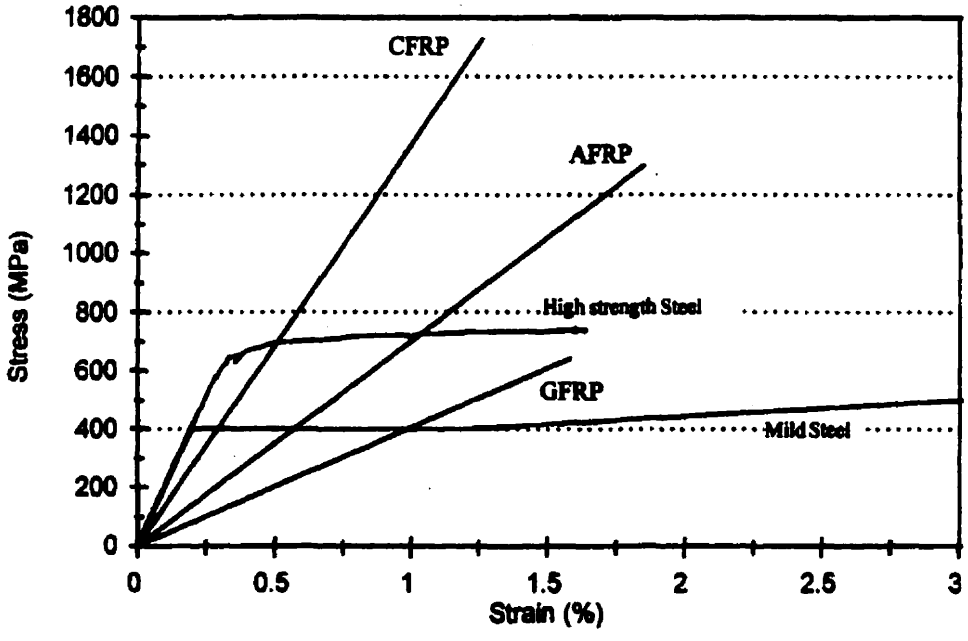

Figure 2-1 Linear stress-strain behaviour of FRP bars

The resin matrix is required to distribute the load within the cross section through the laminate shear mechanism. It also provides a barrier against an adverse environment, and protects the surface of the fibres from mechanical abrasion (Mallick, 1993). The matrix is not required to withstand load in the composite and has weak mechanical characteristics. Matrix behaviour is time-dependent, and is a function of the rate and frequency of load applied and the ambient temperature (Mufti, 1991). The presence of the matrix enhances the resistance to buckling of the composite by surrounding and interacting with the fibres. The matrix must be chosen to complement the fibres being used and to provide adequate protection and separation of the fibres to enhance the overall behaviour of the composite. The thermoset polymer and thermoplastic matrices are the most common types used for civil engineering applications (Abdelrahman and Rizkalla, 1994).

2.1.2 FRP Reinforcements

FRP reinforcement for concrete structures can be in the form of rods or ropes, with the advantages of (Abdelrahman and Rizkalla, 1994):

1. A tensile strength-to-weight ratio in the range of six to ten times greater than steel.
2. Excellent corrosion resistance.
3. Electromagnetic neutrality.
4. Low axial coefficient of thermal expansion, especially for carbon fibre reinforced polymer tendons.

5. A weight of one-seventh to one-fifth that of steel reinforcement of equivalent diameter.

The disadvantages of fibre reinforced polymer rods may include:

1. A cost two to ten times higher than steel.
2. Low strain at fracture.
3. Low modulus of elasticity compared to steel.
4. Low strength perpendicular to the fibres.
5. Low compressive strength.
6. Some fibres are susceptible to ultra violet radiation damage.
7. Some fibres absorb water leading to deterioration.

Despite the burgeoning use of FRP in other fields, its application in structural engineering is not as widespread. This may be due to one or a combination of the following:

1. Absence of codes and specifications.
2. Lack of designer confidence due to little relevant experience and education.
3. Incomplete understanding of material properties and lack of data regarding long term behaviour.

The high initial cost of Fibre Reinforced Polymers is a deterrent in certain applications. However, once maintenance and other factors over the life of a structure are considered in

a direct comparison to steel, the cost can be justified. The use of steel incurs the cost of cathodic protection and the future costs related to the shorter life span of steel which is greatly affected by corrosion. With the longer life of FRP in comparison to steel, the higher initial cost may be less significant in the long term (Erki and Rizkalla, 1994).

2.1.2.1 Aramid FRP Reinforcement

Aramid Fibre Reinforced Polymer (AFRP) tendons are produced in a variety of shapes including braided, spiral wound and rectangular rods. The fibres have a higher modulus of elasticity and lower density than glass fibres but have a lower compressive strength, and high moisture absorption (Mallick, 1993). Three types of fibres are Kevlar, Twaron, and Technora with fibre tensile strengths of 2.65 GPa, 2.8 GPa, and 3.4 GPa respectively. However, as a composite with certain fibre volume ratios the strength is reduced to a range of 0.62 to 1.93 GPa (Dolan, 1993).

Kevlar 49 fibres were patented by the DuPont Company and are used in the making of Fibra rod produced by the Mitsui Construction Company in Japan. This rod has multiple bundles of fibres that are braided together and coated in an epoxy. In some procedures, sand is used on the outer surface to increase the bond with the concrete. Twaron fibres are used for Arapree tendons that are considered the strongest of the AFRP. Hollandsche Beton Groep of the Netherlands produces this type of rod by pultrusion of Twaron fibres and an epoxy

resin. Pultrusion is the process whereby fibres are roughly shaped and pulled through a resin bath and through heated dies followed by a final stage of curing, as shown in Figure 2-2 (Mufti et al., 1991). Technora rod is produced by Teijin Limited of Japan using Technora fibre and a resin combined during the pultrusion process.

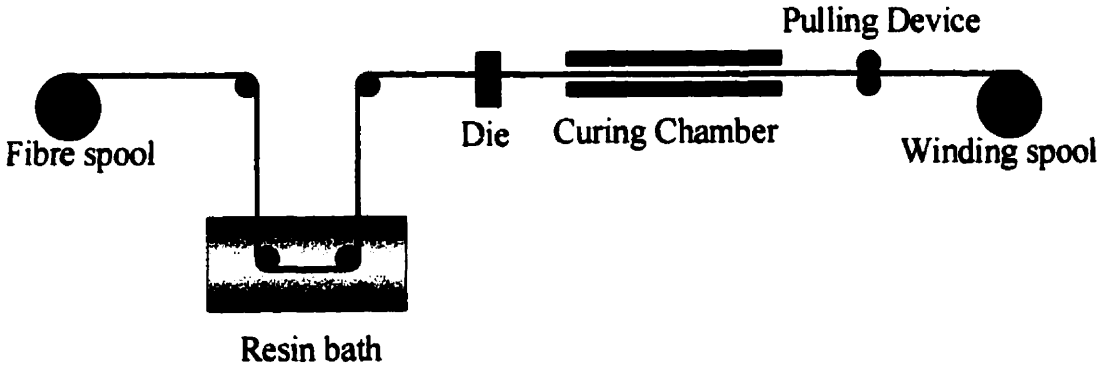

Figure 2-2 Pultrusion process

2.1.2.2 Glass FRP Reinforcement

Glass fibre reinforced polymers are the most economical of all fibre reinforced polymers and are commonly used in low stress level conditions due to their relatively low cost. GFRP, in general, is used for non-prestressed reinforced members. Disadvantages of GFRP include low elastic modulus, relatively high specific gravity (in comparison to other fibres), creep rupture, and lower fatigue resistance (Erki and Rizkalla, 1994).

The two commonly used types of glass fibres are the E-glass and S-glass fibres. S-glass fibres are more expensive than E-glass but are more temperature resistant and have a tensile strength of 3.9 GPa and a tensile modulus of 87 GPa. E-glass fibres have a lower tensile strength of 2.3 GPa and tensile modulus of 74 GPa (Dolan, 1993). The presence of water as well as the application of sustained loads decreases the tensile strength of glass fibres (Abdelrahman and Rizkalla, 1994).

Glass Fibre Reinforced Polymers are typically produced using the pultrusion process. The common industrial name for one type of GFRP bar is Isorod produced by Pultrall Incorporated, Quebec. These bars are manufactured with diameters of 9.5, 12.7, 15.9, 19.1 and 25.4 mm. To improve the bond, external winding (to produce a ribbed surface) is done and quartz sand grains are attached to the surface (Abdelrahman and Rizkalla, 1994).
Another type of GFRP bar is commercially known as C-BAR, produced by Marshall Industries in Lima, Ohio, USA. C-BAR uses E-glass fibres and a polyurethane resin. It is also fabricated using the pultrusion process in the form of straight bars and pre-fabricated stirrup shapes (both single legged and double legged). Both 12 and 15 mm diameter bar sizes are available fabricated with resin ridges to enhance the mechanical bonding to the concrete.

2.1.2.3 Carbon FRP Reinforcement

Carbon fibre reinforced polymers (CFRP) are the most widely used reinforcements due to many beneficial characteristics. They have a very high tensile strength, high fatigue strength, a high modulus of elasticity, and yet low density, and low relaxation. They have the highest elastic moduli of all fibre reinforced polymers, ranging from 125 to 230 GPa.

The Tokyo Rope Manufacturing Company Limited produces Carbon Fibre Composite Cable (CFCC). Carbon fibre pre-pregs, which contain 12,000 filaments embedded in resin, are manufactured by the Toho Rayon Co. Each pre-preg is twisted and then covered by synthetic yarns to create one single strand. A CFCC rope is typically produced in single strands or by twisting larger numbers of strands in combinations of seven, nineteen, or thirty-seven wires as shown in Figure 2-3. This rope can be rolled and shipped in a large roll form. The twisted rope can also be shaped into various stirrup forms before curing. CFCC has excellent bond characteristics to the concrete due to the extra surface area and high relative roughness of the rope (Abdelrahman and Rizkalla, 1994). Some CFCC cables have been fabricated which attain 90% of the carbon fibre strength and 97% of the carbon fibre tensile modulus (Mochizuki et al., 1989).

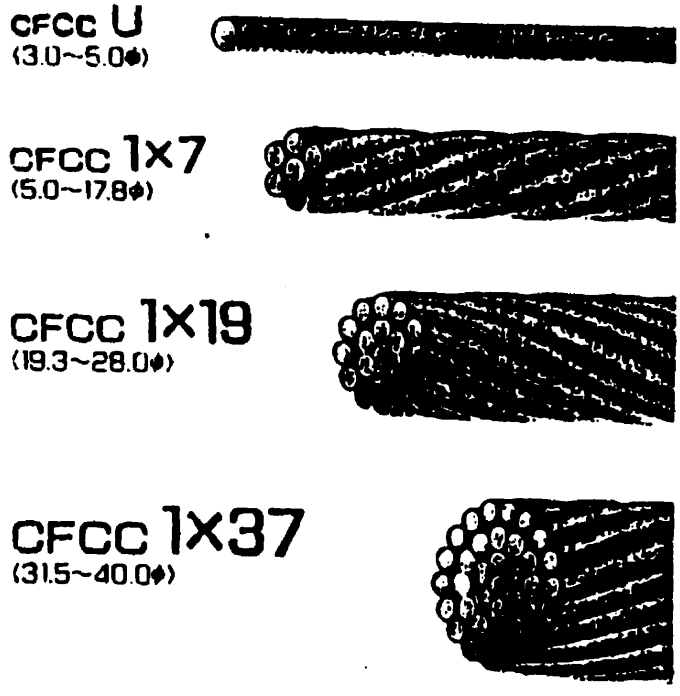

Figure 2-3 CFCC bars in cross-section (Tokyo Rope Manufacturing Company, 1993)

Leadline, produced by the Mitsubishi Chemical Corporation, is another widely used CFRP bar. The pultrusion process is again utilized for the carbon fibres and an epoxy resin to produce the Leadline rods. Leadline can be shipped in reels or coils and then cut for use as a prestressing tendon in beams. It is also produced in stirrup shapes used for shear reinforcement consisting of fibres encased in a resin coating. An 8 mm diameter Leadline prestressing rod has a guaranteed tensile strength and modulus of 1970 MPa and 147 GPa respectively.

2.1.3 Behaviour of Concrete Members Reinforced with FRP

Due to the unique material properties of FRP compared to steel, beams reinforced with FRP behave differently than beams reinforced with traditional steel reinforcement. As previously mentioned, FRP materials have a linearly elastic behaviour up to failure. This behaviour leads to concrete beam failure either by crushing of the concrete in the compression zone or by the brittle failure of the FRP reinforcement. Due to the absence of yielding, beam behaviour and the mode of failure are different from those associated with steel reinforced beams, and therefore special design considerations should be used for the design of concrete structures reinforced or prestressed with Fibre Reinforced Polymers.

2.2 FRP Shear Reinforcement

FRP is easily molded into different stirrup shapes similar to traditional steel stirrups. However, because of its different properties, FRP cannot be directly substituted for steel stirrups in design. Problems are encountered due to the effect of the bends in the stirrups and due to the effect of inclined shear cracks. These problems must be investigated before design guidelines can be developed.

2.2.1 Classification and Fabrication of FRP Stirrups

Different configurations of FRP stirrups are currently available on the market. These range from individual stirrups, similar to traditional steel stirrups, to three-dimensional grids of FRP material. Most of these forms of stirrups are delivered to the site in the desired shape. The following listing describes some of the currently available products and the particular method of fabrication. Different stirrup configurations are shown in Figure 2-4.

The typical pre-bent closed loop stirrups are fabricated using a continuous filament winding process. The material is wound around a mold into one large stirrup. Upon completion of the curing process, the mold is removed and the large stirrups are cut into smaller stirrups of the appropriate width, as described by Duranovic et al (1997).

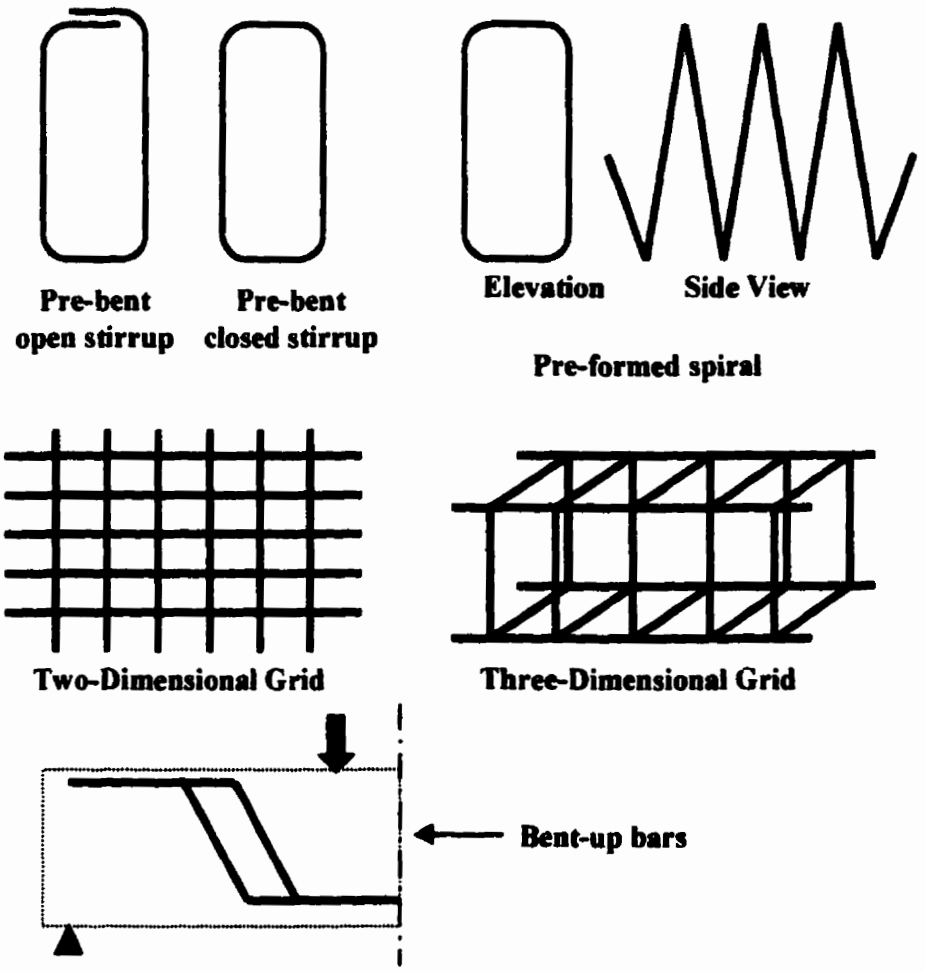

Figure 2-4 Various stirrup configurations

The open loop stirrups used in this experimental program were prefabricated. Instead of being continuous on both ends similar to the closed loop stirrups, they are cut at the compression zone and have a standard hook (lapped) end. Maruyama (1993) reported on two types of bending processes. In the first method, the pre-pregs (resin-impregnated continuous fibre rovings and mat) are bent around metal bars of the required radius and heated for curing. During this process, the configuration of fibres at the bend becomes flattened and consequently the strength is significantly reduced. This imperfect section does not allow full development of the strength of the FRP bar. For this reason another method has been developed to prevent this damage to the stirrup section. The second method allows the cross section to remain circular and there is no flattening of the fibres. The pultruded FRP bars are bent around semi-circular grooved metal molds with a radius equal to the bar diameter. By containing the fibres around the bend, the cross-section is not deformed as the curing process is completed.

Some FRP stirrups are produced in pre-formed spiral shapes, similar to steel reinforcing. Pre-formed spirals are made by continuously winding the FRP pre-pregs into spirals according to the specified dimensions depending on the beam section. This continuous winding process creates long sections which can be cut to the desired dimensions.

FRP reinforcements are also produced similar to steel welded wire fabric in the form of a two dimensional grid. One product currently in production in both Canada and Japan is called NEFMAC. These flat or curved grids were studied by Clarke (1993). To form the two-dimensional grid, a continuous filament winding (pin-winding) process is used to impregnate fibres with resin that is cured with ultraviolet light once formed into the grid shape. This process is generally favourable for grids with small cross sections. To create grids of large cross section, or to construct three-dimensional grids, a batch process is used. Here, a peroxide curing system is used to impregnate the fibres that are formed into the grid shape at room temperature. Three-dimensional grids have been used as cage reinforcement for concrete beams.

2.2.2 Bend Effect

Stirrups are widely used as shear reinforcement in reinforced or prestressed concrete beams. However, to develop the full strength of these stirrups, sufficient anchorage within the beam is required. FRP shear reinforcement has been evaluated by investigating the behaviour of the bend. While the tensile strength of the straight section of the bar may be more than adequate, the strength at the bend is significantly less. Mochizuki (1995) notes that for an end bearing system the strength of the bend is only 30% to 70% of the straight bar strength. By examining an individual fibre, shown in Figure 2-5, it is obvious that the large deformation around sharp bends in the fibres can cause significant reduction of the overall

strength at the bent portion of the rod. At these locations failures occur due to the residual stresses induced by the bending of the fibres leading to a lower strength.

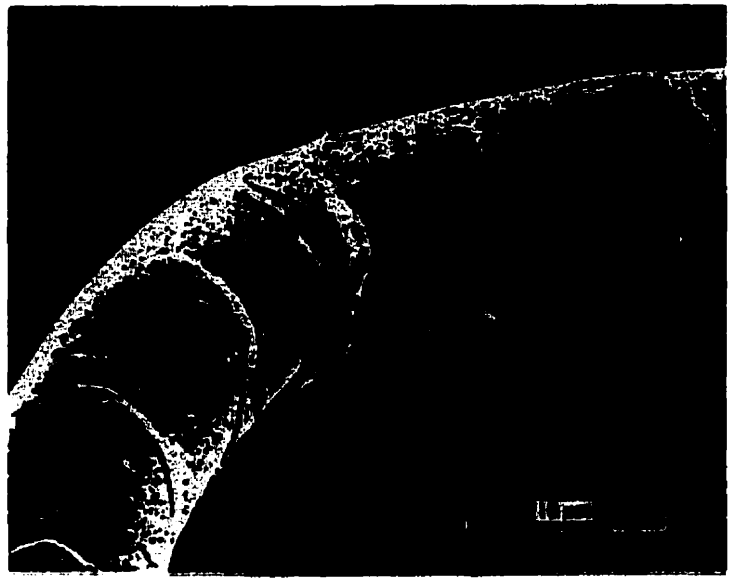

Figure 2-5 Microscopic bent fibre (Hull, 1981)

A diagram showing the stresses at the bend can be seen in Figure 2-6. At the bend location the load is directed perpendicular to the fibre direction. FRPs have lower load carrying capacity perpendicular to the fibres, therefore, the radial stresses at the bend location will cause significant reductions of the strength. The fibre type, bar diameter, embedment length, tail length and bend radius all affect the stress level at the bend and subsequently govern the capacity of FRP stirrups in relation to the stresses at the bend location. The following studies have previously investigated the bend effect.

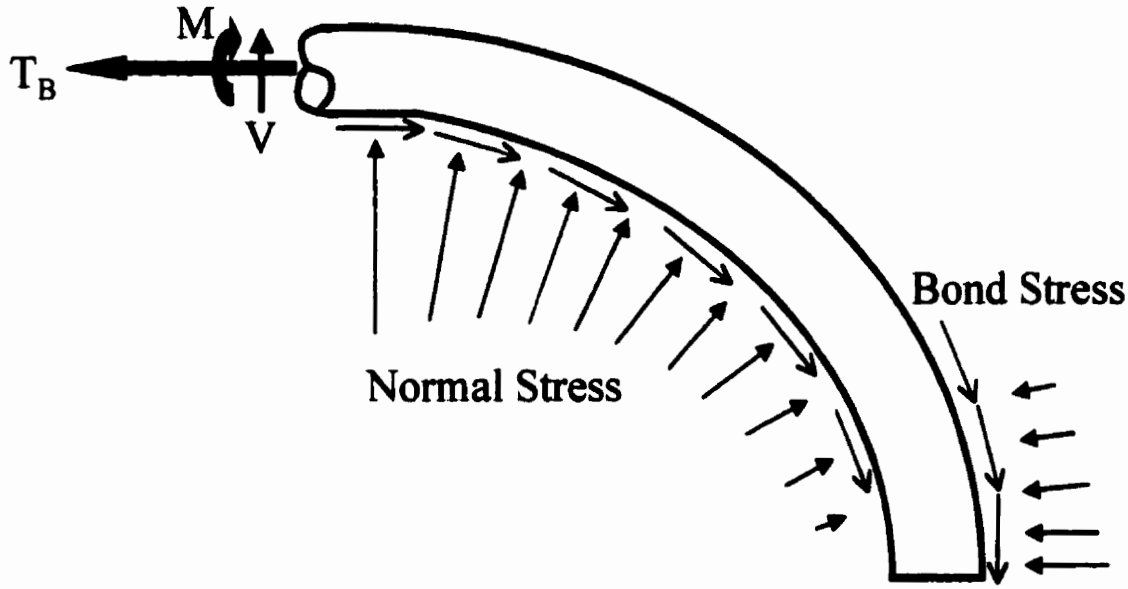

Figure 2-6 Stresses at the location of the bend

Research into the capacity of CFRP and AFRP bent rods was conducted by Maruyama et al (1993). They investigated the tensile strength of bent FRP rods while varying the type of material, the bend radii and the concrete strength. Pultruded CFRP rods, 7-strand CFRP rods, and braided AFRP rods were tested and compared to steel bars. The internal radii considered in this investigation were 5 mm, 15 mm, and 25 mm for each type of rod. Both high strength concrete (50 MPa) and ultra high strength concrete (100 MPa) were used with the different FRP rods. The bend was embedded in concrete at an embedment length of 50 mm and tension was applied to the rod using a 150 kN hydraulic jack, as shown in Figure 2-7.

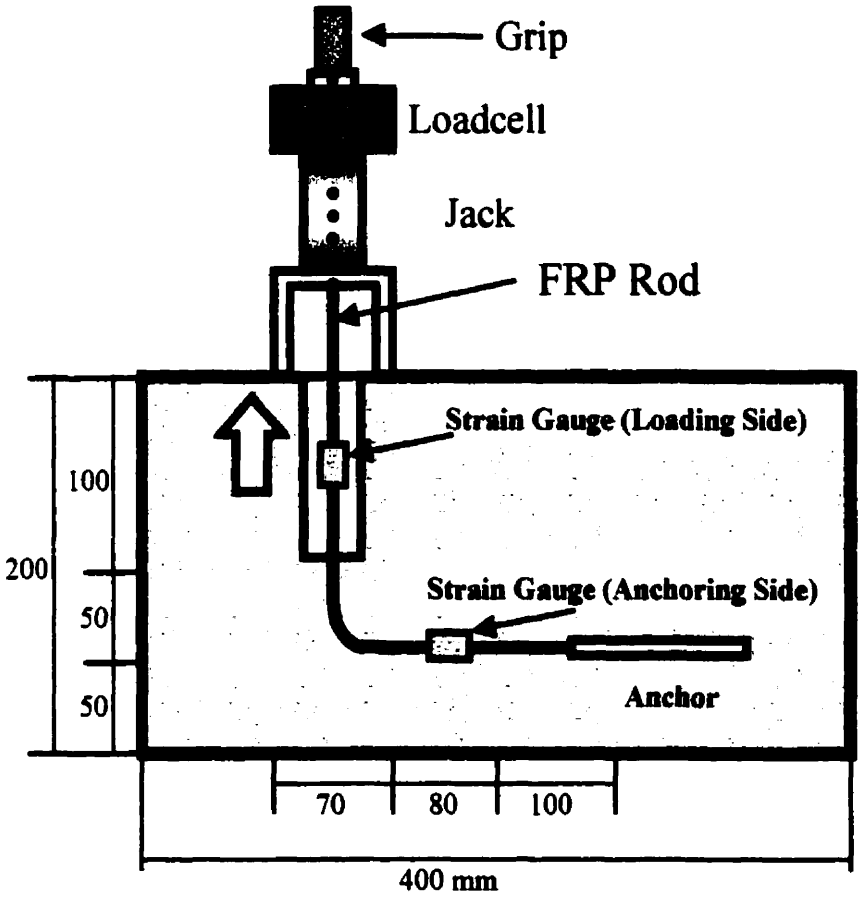

Figure 2-7 Bent bar test specimen of Maruyama et al (1993)

The researchers found that all CFRP and AFRP rods failed at the bend. They also discovered that decreasing the radius of the bend decreased the tensile strength in a hyperbolic relationship. As the bend radius decreased, the tensile force transferred around the bend to the anchored portion increased. With a higher stress at the bend, the strength is reduced. The type of rod as well as bending method affected the degree of increase of this transfer. Use

of high strength concrete increased the strength of FRP at the bend.

Hooked GFRP bars were studied by Ehsani et al (1995). They examined the relationship between the bar strength and the concrete compressive strength which was varied from 28 to 56 MPa. The other parameters included in this study were the ratio of bend radius to bar diameter, the bar diameter (9.5, 19.0, 28.6 mm), tail length beyond the hook, and straight embedment length before the hook. The research work included thirty-six specimens tested with GFRP bars encased in concrete blocks. The load was applied through a special sand coated gripping system, which caused shear lag between the outer fibres and the inner fibres, especially for bars of large diameter. This setup is shown in Figure 2-8. Evaluation of the various parameters was based on the loaded end slip, failure load, mode of failure, and initial stiffness. The initial stiffness was determined using the secant modulus of the load-slip relationship as shown in Figure 2-9. The load-slip relationship was corrected by excluding the elastic extension of the bar along the unbonded portion within the concrete (3 in.) and the portion outside of the concrete block (4 in.) from the measured slip.

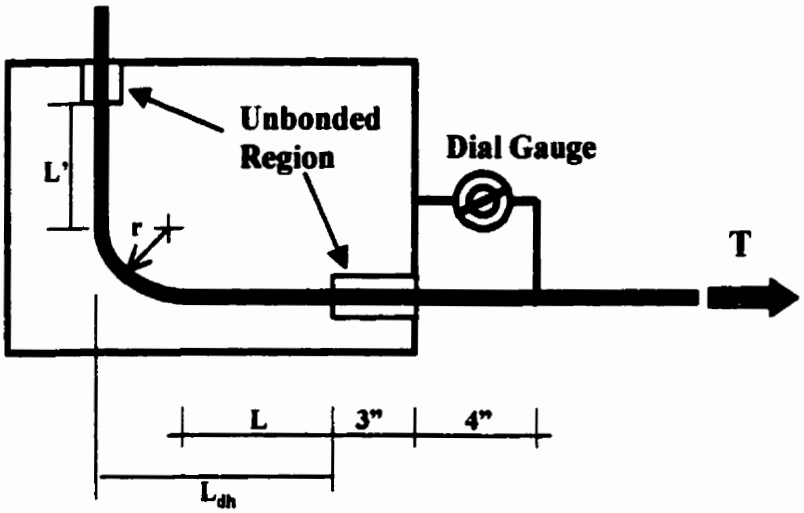

Figure 2-8 Bent bar test specimen of Ehsani et al (1995)

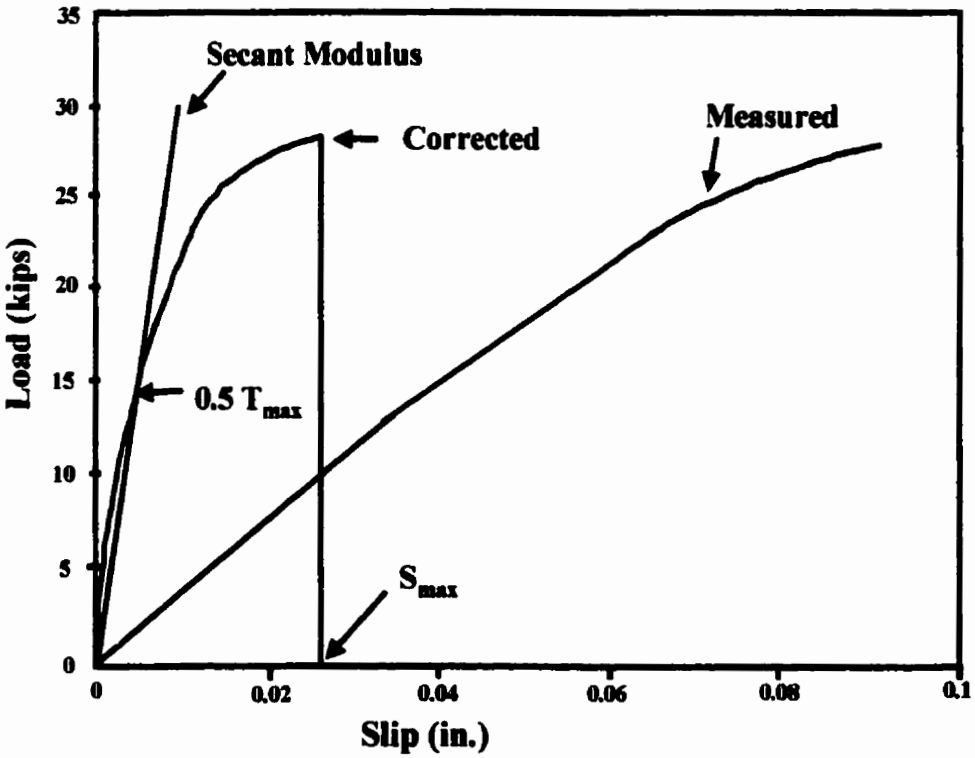

Figure 2-9 Secant modulus used by Ehsani et al (1995)

The researchers found that using large diameter GFRP bars caused splitting of the concrete blocks. Test results indicated that the capacity was reduced at the bend as predicted and was affected by the bend radius and the bar diameter. The capacity ranged from 64 to 70% of the strength parallel to the fibres for bar diameters of 9.5, 19.0 and 28.6 mm using a bend radius of $3d_b$. These strengths decreased further, to 15, 16 and 18% for bar diameters of 9.5, 19.0 and 28.6 at a bend radius equal to zero. They recommended a minimum bend diameter of $3d_b$ for GFRP hooks and a tail length of $12d_b$. As the straight embedment length of the bar increased, the tensile strength and the initial stiffness also increased. A total development length of $16d_b$ was recommended for the 90° GFRP hooks.

Currier et al (1993) investigated the bond development strength and failure modes of FRP stirrups as shear reinforcement. They tested both Nylon/Carbon and Nylon/Aramid stirrups with a cross sectional area of 17 mm^2 and a fibre volume of 50%. Two stirrups were placed one above the other and the two ends were cast in concrete blocks 125 mm x 150 mm x 150 mm. The stirrups were tested to failure in tension applied by a hydraulic jack located with a load cell in between the two concrete blocks, as shown in Figure 2-10.

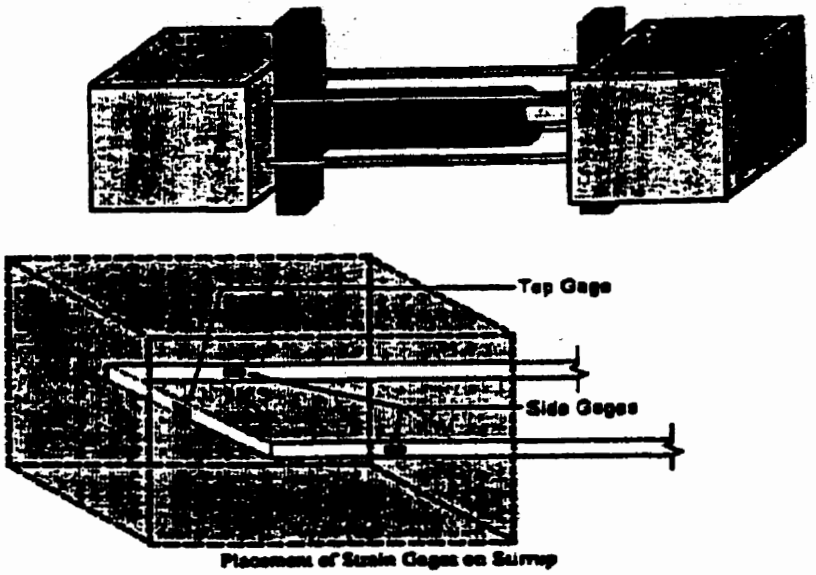

Figure 2-10 Stirrup bend effect test specimen of Currier et al (1993)

For the Nylon/Carbon stirrups, losses in strength were observed, as predicted, due to the bend effect. The ultimate stress capacity was found to be 23% of a similar straight bar, due to failures at the bend location. The researchers concluded that the strength of the stirrup was only 25 percent of the ultimate strength of the Nylon/Carbon bar. Increasing the bend radius of the stirrup from the 12.7 mm radius used may have prevented failure at the bend. The Nylon/Carbon stirrups were found to perform poorly when compared to the Nylon/Aramid stirrups, due to their poor capability to resist loading transverse to the fibres.

Nakamura and Higai (1995) conducted a theoretical investigation of the bend capacity of FRP stirrups. They proposed an equation for the bent bar strength shown as Equation 2-1. Under a tensile force with no concrete-FRP bonding, the FRP bar will stretch Δx uniformly across the cross section in the straight portion of the bar subjected to the uniform axial force. It is assumed that a corner radius of r is maintained through a cross section deformation at a rotation angle of ϕ (rad). Using the Bernoulli assumption, a hyperbolic curve represents the strain distribution in the cross section. The corresponding stress distribution can be found by multiplying the strain by the elastic modulus E_{frp}. Equation 2-1 for the bent bar strength capacity is then obtained by integrating the stress distribution over the cross section, with d_b being the height of the rectangular cross section and r_b the bend radius of the section. This relationship is plotted and compared to experimental results in Figure 2-11.

$$\frac{f_{fv}}{f_{fuv}} = \frac{r_b}{d_b} \ln\left(1 + \frac{d_b}{r_b}\right) \qquad (2\text{-}1)$$

where,

f_{fv}	=	ultimate stress achieved experimentally
f_{fuv}	=	ultimate guaranteed strength
r_b	=	bend radius
d_b	=	bar diameter

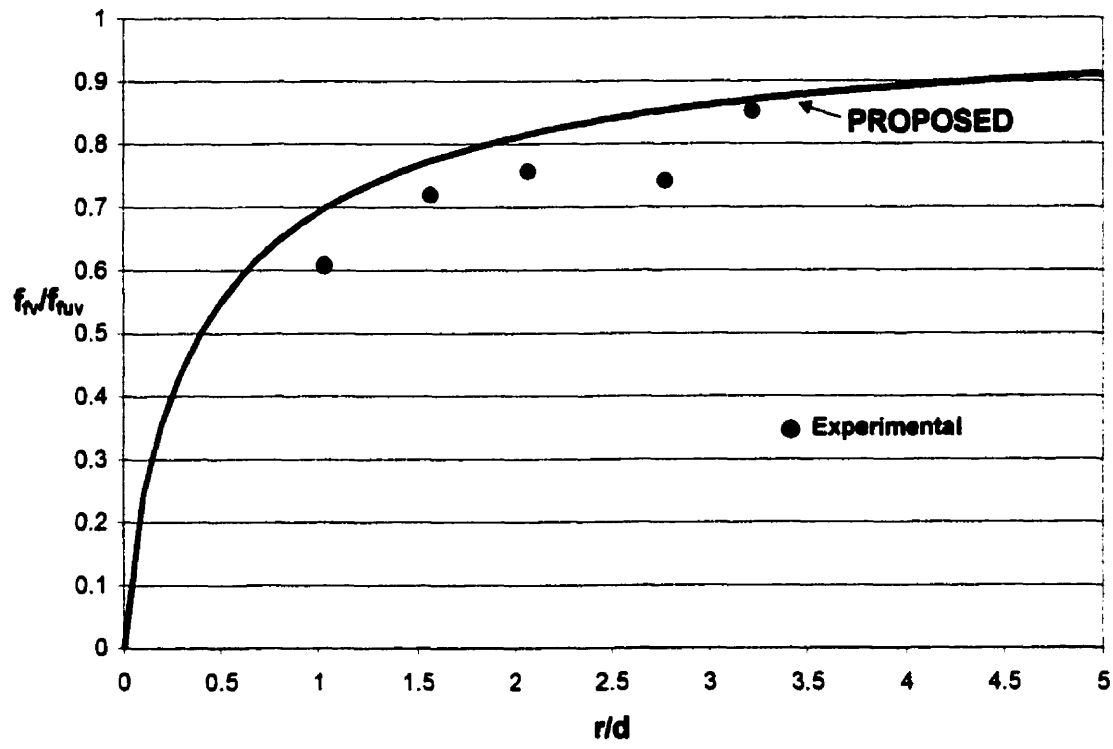

Figure 2-11 Proposed equation for bent capacity from Nakamura & Higai (1995)

FRP stirrups were evaluated by Ueda et al (1995) in terms of their failure criteria and capacity. Aramid fibre stirrups were used in a configuration simulating the intersection of a closed stirrup with a shear crack, artificially initiated with a 0.5mm thick plastic plate, as shown in Figure 2-12. This FRP material had a cross sectional area of 25 mm^2, a nominal diameter of 6 mm, and a nominal strength of 2560 MPa in the direction of the fibres. The main variable in this study was the embedment length, or the length between the artificial crack and the bend. The lengths used were 10 mm, 60 mm, and 110 mm. In conjunction with the testing program, a 2-D non-linear finite element analysis was conducted to

determine the local stresses at the location of the bend.

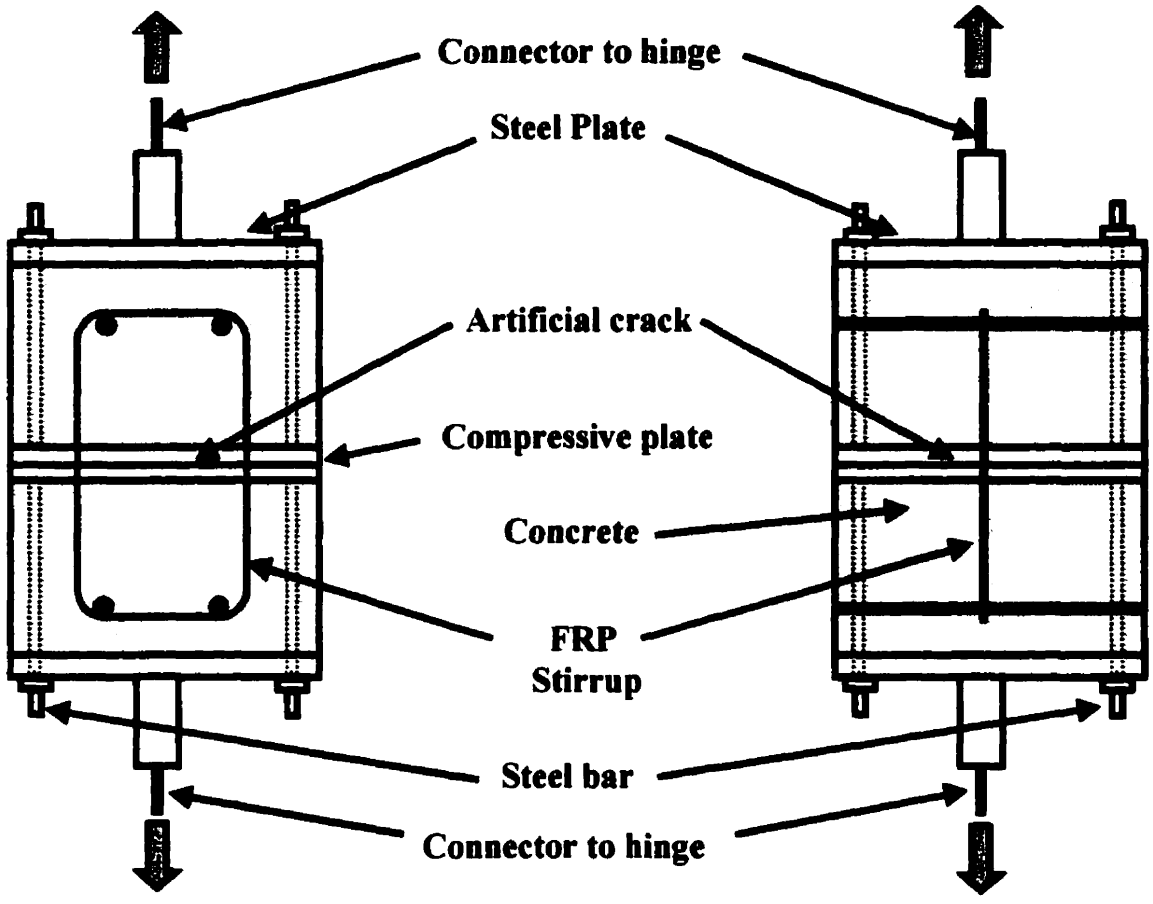

Figure 2-12 Bend capacity test specimen of Ueda (1995)

The results show that the stirrup capacity varied between 41 and 100 percent of the capacity in the direction of the fibres for embedment lengths of 10 and 60 mm respectively. These failures occurred at the location of the bend. Strain increased from the inside surface of the bend to the outside surface. With an embedment length of 110 mm the failure load was increased beyond the nominal strength of the straight bar.

FIBRA FRP bars were investigated by Ishihara et al (1997) to determine the ultimate capacity of FRP stirrups as affected by the bend. They also conducted a finite element analysis to determine the local stresses in the FRP bars at the bend. The test specimens are similar to the ones used in the study conducted by Ueda et al.(1995). Some of the FIBRA bars were made from aramid fibres, while other bars were made from carbon fibres which were twisted together, soaked in resin and bonded with sand on the surface. The bar diameter was 9 mm in both materials and the nominal strengths in the direction of the fibres were 100.3 kN for the AFRP bars and 143.8 kN for the CFRP bars. Three bend radii were used for both materials of 9 mm, 27 mm, and 45 mm which are equal to one, three and five times the bar diameter respectively. Another variable in this study was the stirrup bond length within the concrete, with the debonding extending from the location of the artificial crack to where the bend begins. Four specimens of each material were tested in conjunction with the finite element analysis.

The researchers found that as the bend radius decreases, the stirrup strength also decreases. The strength reduction due to the bend varied depending on the material used, as a result of the different bond characteristics. The bonded specimens showed a strength capacity ranging from 60 percent to 86 percent of the strength in the direction of the fibres for the AFRP bars and 49 percent to 66 percent for the CFRP bars. From the finite element analysis, the capacity of the bend can be predicted using equation 2-2 derived for a rectangular cross

section (but which can be applied to circular cross sections):

With,

$$\frac{f_{fv}}{f_{fuv}} = \frac{1}{\lambda}\ln(1+\lambda) \qquad (2\text{-}2)$$

$$\ln\lambda = 0.90 + 0.73\ln\left(\frac{d_b}{r_b}\right)$$

d_b = bar diameter

r_b = bend radius

2.2.3 Inclined Crack Effect

The second major effect which could lower the capacity of FRP stirrups used in concrete members is the inclined crack effect. This phenomenon occurs when a vertical stirrup crosses an inclined shear crack. As the crack widens, the stirrup crossing this crack is subjected to a kinking action, as shown in the diagram in Figure 2-13. This movement loads the stirrup in a direction out of line with the fibre direction and therefore can cause a reduction in strength.

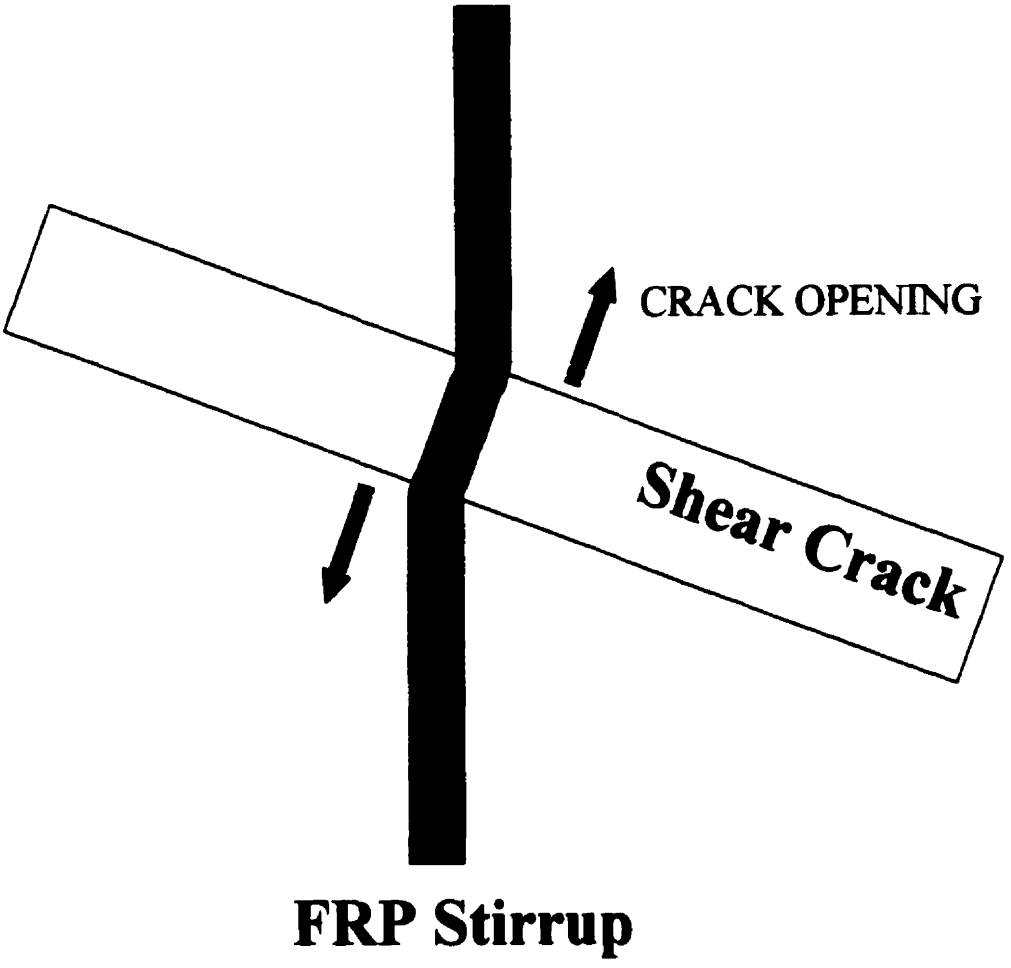

Figure 2-13 Diagram of kinking behaviour

Maruyama et al (1989) studied the effect of the direction of the crack relative to the FRP bars. The researchers used three types of FRP bars in their study, namely carbon, aramid, and glass fibres in an epoxy resin matrix. These bars, with nominal diameters of 5, and 6 mm, all had tensile strengths greater than 1500 MPa. The FRP stirrups were cast into concrete blocks, as shown in Figure 2-14, with an initiated crack of varying angles up to 30

degrees. A hydraulic jack was used to load the specimen subjecting the stirrup to shear forces similar to the forces induced in a stirrup located across a diagonal crack. The results showed that the tensile capacity of FRP bars was reduced significantly by increasing the angle of the applied load with respect to the fibre direction. The angle θ of the FRP bar can be used to determine the reduced strength of the bar f_{fv} with respect to the direction of the fibres and the strength in the direction of the fibres f_{fuv}, using equation 2-3:

$$f_{fv} = f_{fuv}\left(1 - \frac{k}{100}\theta\right) \qquad (2\text{-}3)$$

where k is the reduction factor and has a value range of 1.9 to 2.3 for CFRP bars, 1.9 for AFRP bars, 1.3 for GFRP bars and 0.1 for steel. This applies for angles of θ between zero and 30 degrees. Using the provided equation, the diagonal stirrup tensile strength at the maximum angle of 30 degrees is 30% of the strength in the direction of the fibres for CFRP, 45% for AFRP and 65% for GFRP.

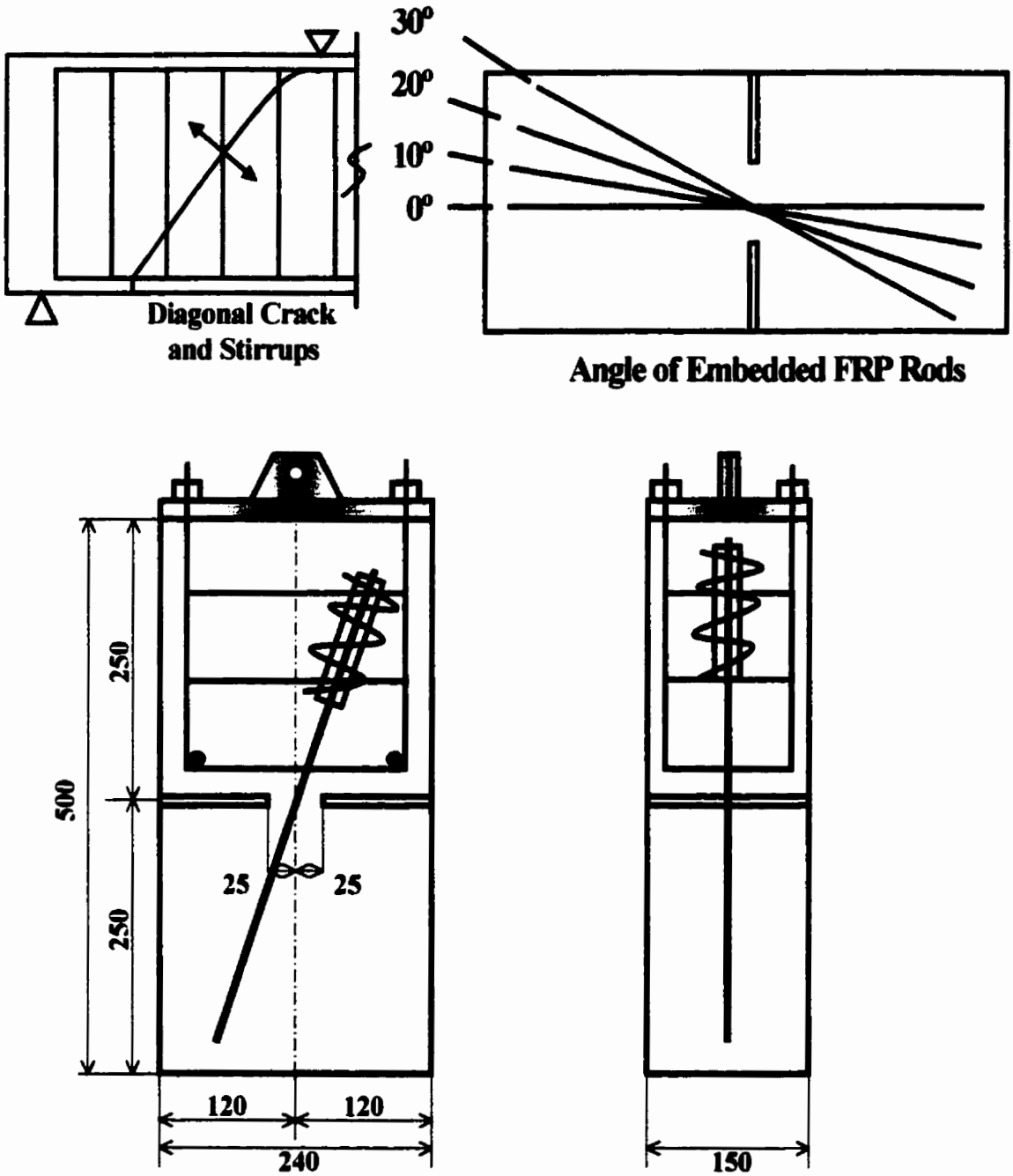

Figure 2-14(a) Angled bar test specimen of Maruyama et al (1989)

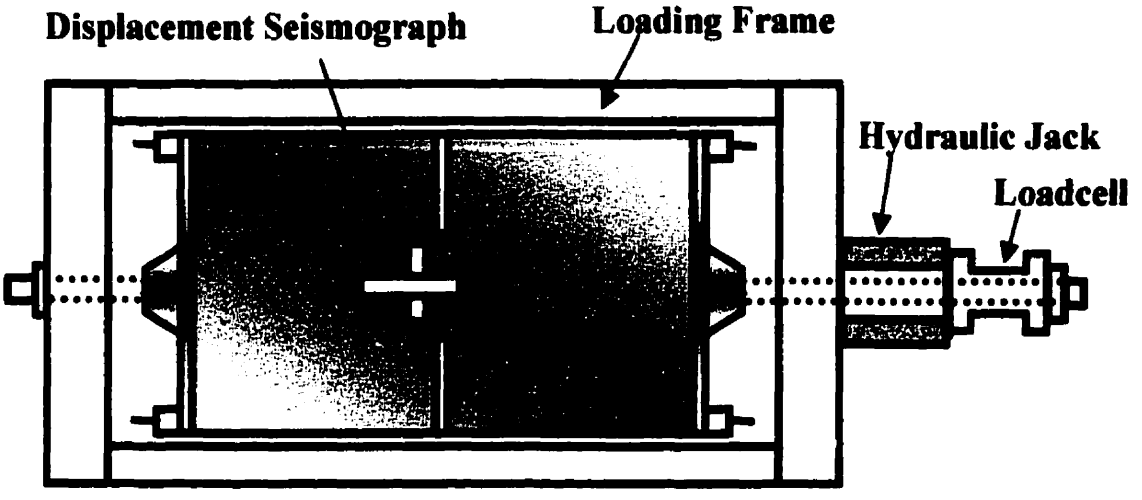

Figure 2-14(b) Angled bar test specimen of Maruyama et al (1989)

Two groups of researchers, Kanematsu et al. (1993) and Ueda et al. (1995), studied the effects of combined tensile and shear forces on AFRP bars using specially designed concrete block specimens. These bars had an 8 mm nominal diameter, a tensile strength of 1280 MPa and an elastic modulus of 65 GPa. The FRP was located at the center as shown in Figure 2-15, and the blocks were separated into three parts by stainless steel plates. Tension was applied to the FRP through the separation of the blocks under loading from the hydraulic jack. When the specified crack width was reached, the end blocks were fixed in place to hold this width constant. An independent hydraulic jack was used to load the middle block laterally which subjected the tensioned FRP bar to shear displacement and shear force. The crack width was varied in the different specimens. Kanematsu et al. (1993) reported four

specimens and Ueda et al. (1995) reported a further eight specimens. In addition, 3-D linear finite element and 2-D non-linear finite element analyses were conducted investigating the local stresses in the AFRP bar at the location of the crack.

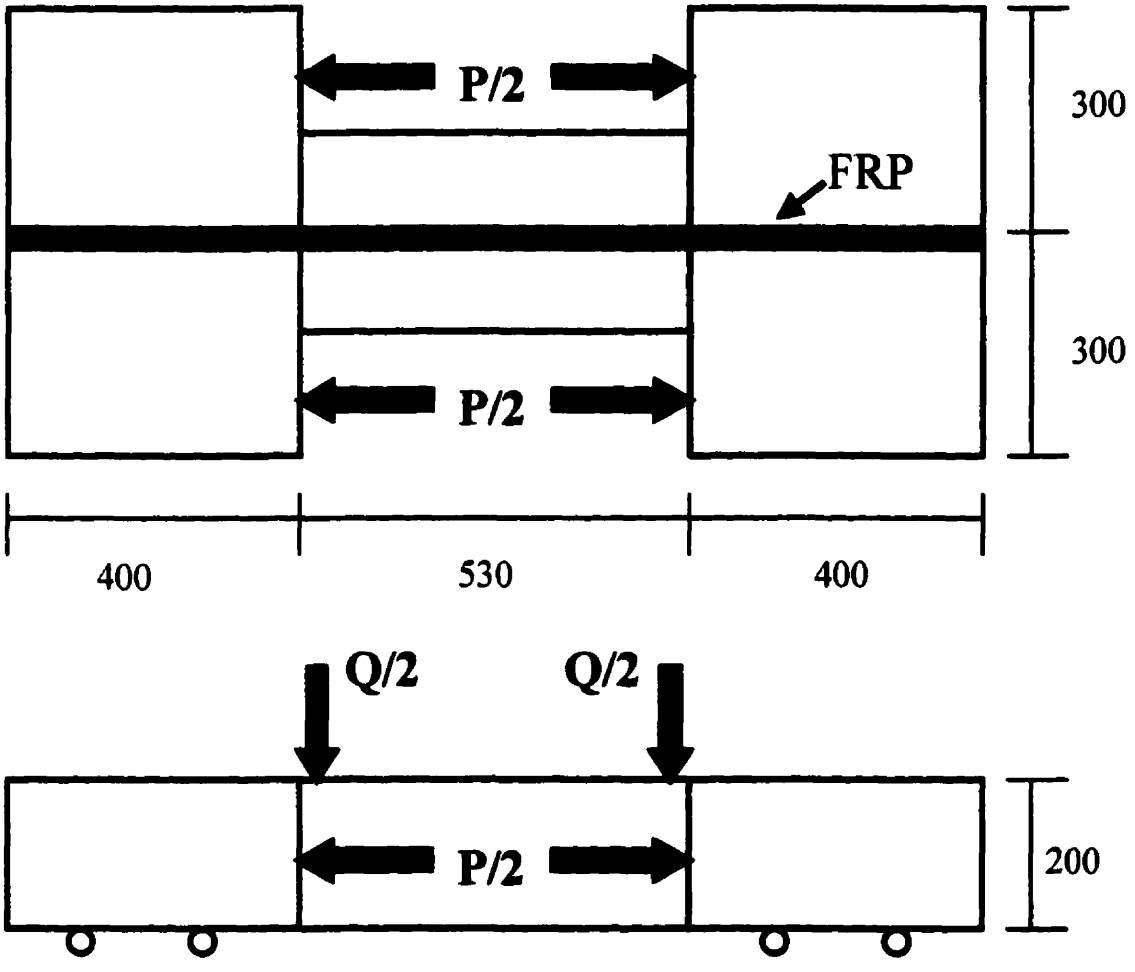

P = Tension force

Q = Shear force

Figure 2-15 Combined tension and shear test specimen of Kanematsu & Ueda (1993/1995)

The researchers found that the tensile strength of the AFRP bar was reduced significantly at the crack location due to the combined action of the tensile and shear forces. They recommended that in addition to considering tensile and shear forces in the FRP bar for the failure criteria, crack width and shear displacement should also be considered. To determine the strength of the stirrups at the crack location using the finite element models, reasonable assumptions must be made for: (a) the FRP bar's shear modulus; (b) the debonding length around the FRP bar at the crack location; and (c) the bond stress-slip relation of the FRP bar.

Nakamura and Higai (1995) completed a theoretical study of the diagonal tension strengths of FRP bars. Their model considered a tensile force applied to an FRP bar of length L at an angle of θ with respect to the direction of the fibres. With L as the length of intersection between the FRP and the diagonal crack of angle θ, the following equation was derived for the diagonal tensile strength of a rectangular section:

$$f_{fv} = \frac{f_{fuv}}{\cos\theta + 6\sin\theta\tan\theta} \qquad (2\text{-}4)$$

As well, they provided an equation for circular sections,

$$f_{fv} = \frac{f_{fuv}}{\cos\theta + 8\sin\theta\tan\theta} \qquad (2\text{-}5)$$

In comparison to the work done by Maruyama et al (1989), the proposed equations were shown to be reasonable in evaluating the strength reduction due to the diagonal tensile force. However, these equations do not consider the effects of fibre type, despite the fact that the reductions have been shown to be dependent on the type of fibre used in experimentation.

CHAPTER 3: EXPERIMENTAL PROGRAM

3.1 General

The two-phase experimental program was designed to determine the strength of FRP stirrups as shear reinforcement for concrete structures. The first phase investigated the strength of FRP stirrups as affected by bending FRP bars into stirrup configuration. The parameters considered in this phase were the material type, radius of bend, bar diameter, anchorage conditions, tail length, and embedment length. One hundred and one specimens were tested.

In the second phase, twelve specimens were constructed and tested to evaluate the effect of inclined cracks on the stirrup capacity. The two parameters in this phase were the material type and the crack angle with respect to the stirrup. This chapter describes the material properties, specimen fabrication, test set-up, instrumentation and test procedure used for each phase.

3.2 Materials

For both experimental phases, CFRP and GFRP stirrups were used, with steel stirrups as control specimens. The two types of CFRP stirrups used were Leadline and Carbon Fibre Composite Cable (CFCC). The GFRP stirrups used were C-BAR. The properties of all stirrups used are shown in Table 3-1, while Figure 3-1 shows a photograph of these different

stirrups. CFRP bars, in comparison to other commercially available FRP bars, have the highest tensile strength, the highest tensile elastic modulus, however they exhibit the lowest strain at failure. GFRP bars are the most economical, have a low tensile elastic modulus but have a high tensile strain in comparison to other FRP bars.

Table 3-1 Material properties of FRP and steel stirrups

Type of Bar	CFRP	CFCC			GFRP	Deformed
	Leadline bar	U - 5.0	7-wire	7-wire	C-BAR	Steel bar
Nominal diameter d_b (mm)	rect. sec. (5x10mm)	5.0	5.0	7.5	12.0	6.35
Nominal area A_b (mm^2)	38.48	15.20	10.10	30.40	113	31.67
Guaranteed strength f_{fg} (MPa)	1800	1842	1782	1875	713	600*
Ultimate tensile strength f_{fu}	1730**	2170**	1810**	1910**	640**	660**
Elastic modulus E (GPa)	140	143	137	137	42	206
Maximum strain ϵ_{fu} (%)	1.3	1.5	1.5	1.5	1.8	> 2.0

* yield strength **based on tension tests

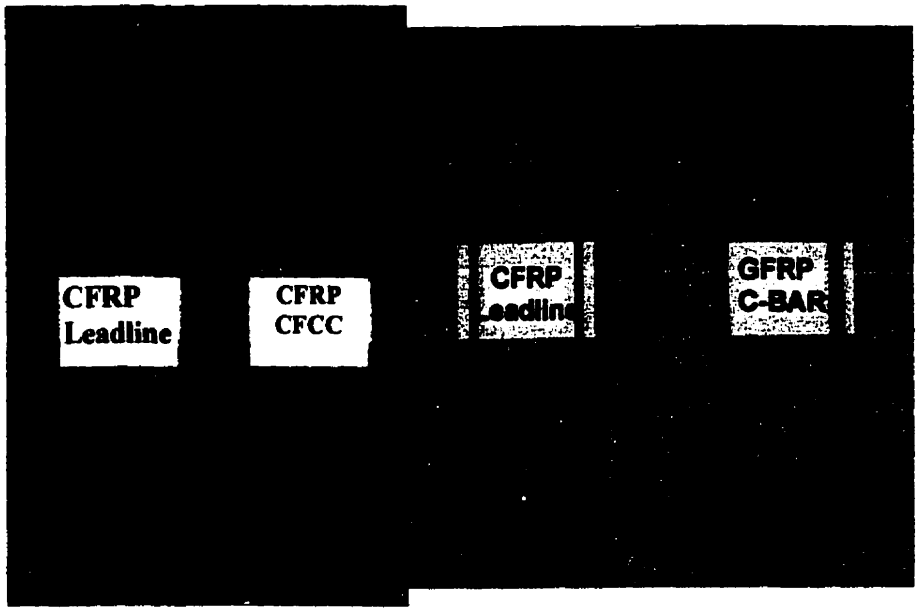

Figure 3-1 Stirrup appearance

3.2.1 Leadline

The Mitsubishi Chemical Corporation from Japan produces the Leadline stirrups used in this study. Leadline stirrup bars are rectangular with a cross-section measuring 5 x 10 mm with a 1 mm resin ribbed coating on the outside surface to protect the fibres from damage. The fibre cross sectional area is 38.5 mm^2, from which an effective diameter, d_e, of 7.0 mm can be found based on Equation 3-1.

$$d_e = \sqrt{\frac{4A}{\pi}} \qquad (3\text{-}1)$$

The stirrups were pre-fabricated in two configurations for testing as shown in Figure 3-2. The inner radius of the bend, r_b, was either 20 mm or 50 mm providing r_b/d_e ratios of 3.0 and 7.0 respectively. Testing of tensile specimens in the R.W. McQuade Structures Lab produced an average tensile stress of 1730 MPa and tensile strain of 1.26 percent at ultimate.

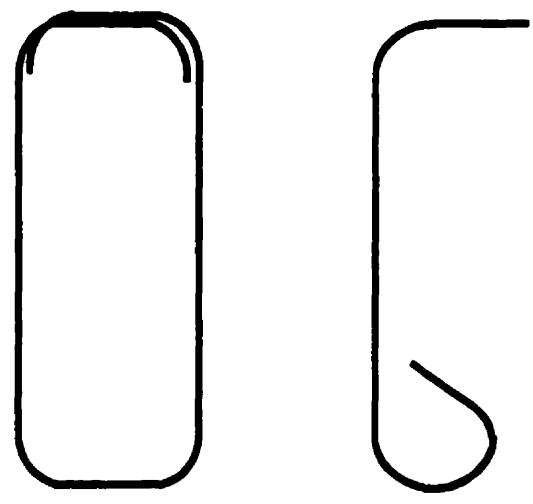

Figure 3-2 Leadline Stirrup configuration

3.2.2 Carbon Fibre Composite Cable

Carbon Fibre Composite Cable (CFCC) is produced by the Tokyo Rope Manufacturing Company Ltd. from Japan. The three bar types used in this study were a seven-wire strand bar with a 7.5 mm diameter, a seven-wire strand bar with a 5 mm diameter, and a solid single wire bar of 5 mm diameter. The inner bend radius of the CFCC stirrups varied,

providing r_b/d_e ratios between 3.2 and 4.8. Tensile specimens were cut from stirrups and tension tests were performed. The results are given in Table 3-1.

3.2.3 C-BAR

C-BAR stirrups are produced by Marshall Industries Composites in Lima, Ohio, USA. The bars used in this study had a nominal diameter of 12 mm and a cross sectional area of 113 mm^2. The inside bend radius of these stirrups was 50mm, which provided a r_b/d_e ratio of 4.0. In multiple tests performed at the University of Manitoba as part of a comprehensive materials testing program, the ultimate tensile stress for C-BAR was 640 MPa, as shown in Table 3-1. This was lower than the guaranteed strength of 713 MPa supplied by the manufacturer.

3.2.4 Steel

The deformed steel stirrups used in all control specimens were supplied by Cowin Steel Company in Winnipeg, Manitoba. The stirrups had a diameter of 6.35mm and a nominal yield stress of 600 MPa. Test results showed a yielding stress of 660 MPa.

3.2.5 Concrete

All specimens were fabricated at the R.W. McQuade Structural Laboratory at the University of Manitoba using concrete provided by Perimeter Concrete. The concrete had a specified maximum aggregate size of 10 mm and a slump of 100 mm with a water cement ratio of 0.40 and a cement content of 330 kg/m^3. Concrete cylinders were tested at the same time as the testing of the specimens, providing an average compressive strength ranging from 36 to 48 MPa. Splitting tension tests produced an average tensile strength ranging from 3.0 to 4.0 MPa.

3.3 Phase 1 – Bend Specimens

The specimens in this phase were specially designed to investigate the effect of the bend on the strength of the FRP stirrups. The location of a stirrup with respect to a shear crack in a beam is shown in Figure 3-3. Figure 3-4 shows a magnified view of the stresses at the bend location.

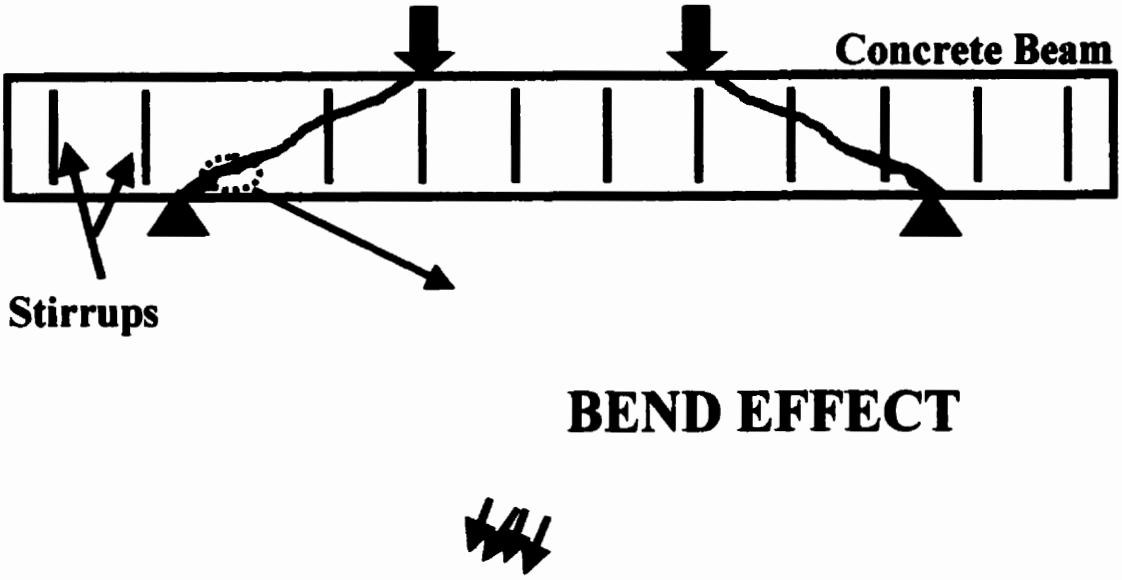

Figure 3-3 Relationship of stirrups to shear cracks producing the bend effect

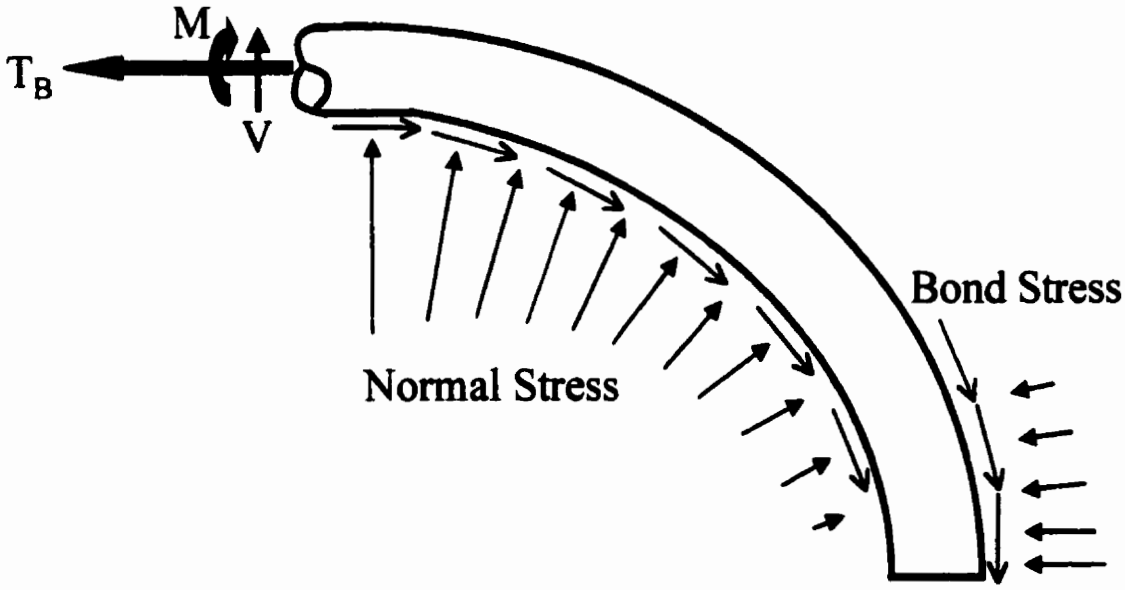

Figure 3-4 Stresses on stirrup at bend location

One hundred and one specimens were constructed using CFCC, Leadline, C-BAR stirrups as well as steel stirrups for control specimens. The parameters for this phase of the testing program, as shown in Figure 3-5, were:

1. Material type - CFRP: Leadline, CFCC 7-wire 7.5mm, CFCC 7-wire 5.0mm, and CFCC single wire

   GFRP: C-BAR

   Steel

2. Embedment length, l_d - Length measured from end of debonding to end of the stirrup, which was varied from 25 to 350 mm.

3. Bend radius, r_b - Radius of the bent portion of the stirrup.

4. Effective bar diameter, $d_e = \sqrt{4 * A/\pi}$

   - Based on the nominal bar cross-sectional area.

5. End Anchorage Type - Type A lapped anchorage (lapped) with a tail length, l_d*, or Type B continuous anchorage.

6. Tail length l_d* - Length of lapped end measured from the end of the bent corner.

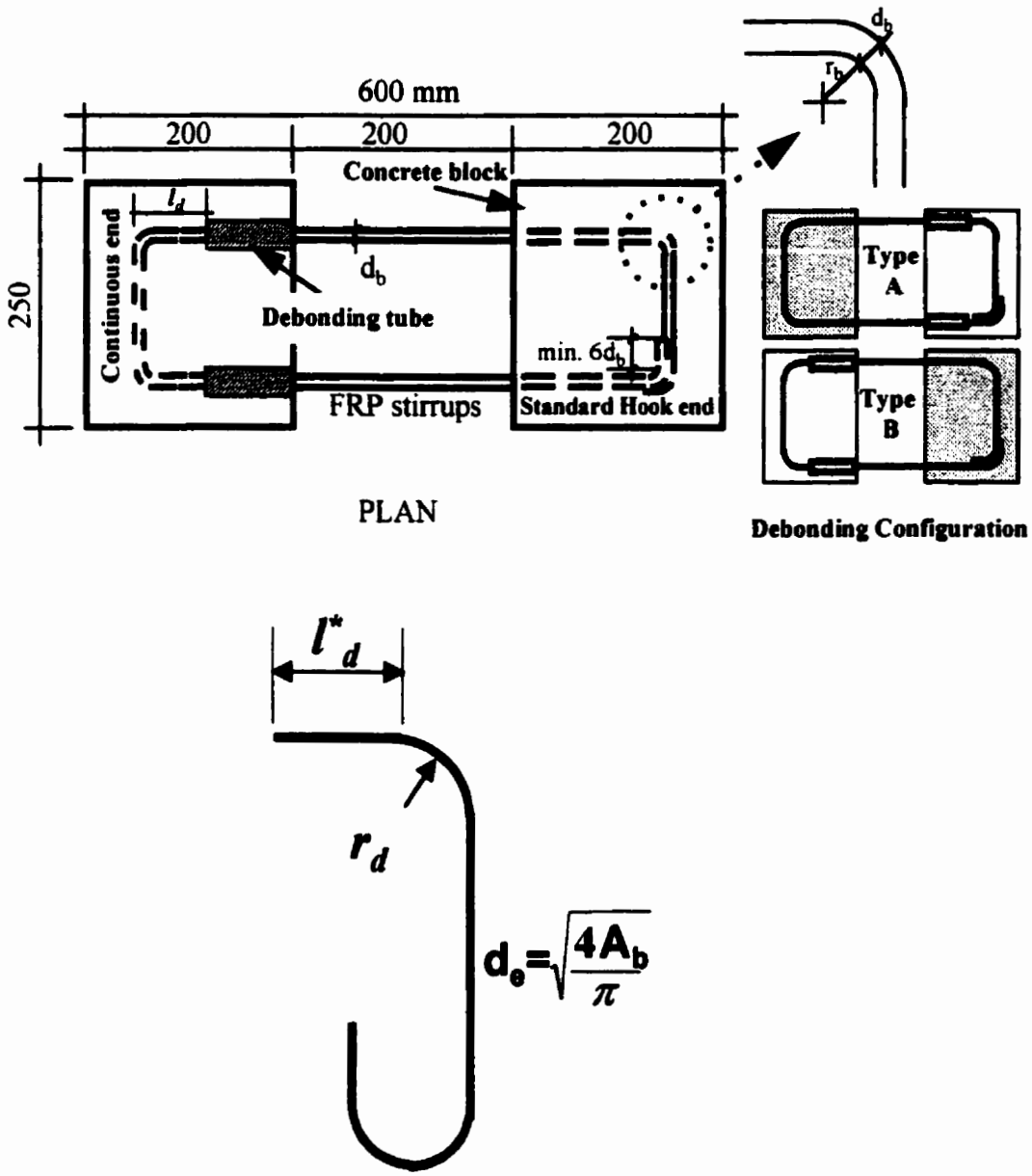

Figure 3-5 Bend specimen configuration

3.3.1 Specimen Design & Fabrication

The stirrups were placed horizontally in the form and concrete blocks were cast around each end as shown in Figure 3-5. This anchorage within the concrete simulates the anchorage of the stirrup within a beam. Type A anchorages (lapped end) are found in the compression zone of a concrete beam, whereas Type B anchorages (continuous end) are found in the tensile zone. The concrete blocks measured 200 x 250 x 200 mm, 300 x 300 x 150 mm, or 500 x 300 x 150 mm, based on the stirrup dimensions plus a 50 mm concrete cover. All of the specimens had a 200 mm clear span between the two blocks for the insertion of a hydraulic jack and load cell.

The embedment length l_d was measured from the end of the stirrup to the beginning of the debonded zone. Plastic PVC pipe was placed around the stirrup leg and sealed at the ends with plasticine to create this debonded length. The other variables are shown in Figure 3-5, and all specimens are detailed in Tables 3-2, 3-3, 3-4, and 3-5.

Table 3-2 Leadline specimens

Material	Bend Radius r_b	Bend Radius r_b/d_e	l_d^* (mm)	l_d (mm)	Stirrup Anchorage Type
Leadline	20	3	21($3d_e$)	r_b+d_b	A
			42	150	
				r_b+d_b	
			63	r_b+d_b	
			84	150	
				r_b+d_b	
			120	r_b+d_b	
			---	150	B
				100	
				r_b+d_b	
	50	7	21 ($3d_e$)	150	A
				r_b+d_b	
			42	150	
				r_b+d_b	
			63	150	
				r_b+d_b	
			84	150	
				r_b+d_b	
			120 ($18d_e$)	350	
				300	
				250	
				150	
				r_b+d_b	
			---	150	B
				100	
				r_b+d_b	
Leadline straight	N/A	N/A	N/A	300	N/A
				150	

Table 3-3(a) CFCC 1x7 5 mm diameter specimens

Material	Bend Radius r_b	Bend Radius r_b/d_e	l_d* (mm)	l_d (mm)	Stirrup Anchorage Type
CFCC	15	4.2	45 ($9d_b$)	150*	A
				80	
				r_b+d_b	
				150*	B
				80	
				r_b+d_b	

*reported for both type A and type B specimen configurations

Table 3-3(b) CFCC single wire 5 mm diameter specimens

Material	Bend Radius r_b	Bend Radius r_b/d_e	l_d* (mm)	l_d (mm)	Stirrup Anchorage Type
CFCC	15	4.2	45 ($9d_b$)	150*	A
				80	
				r_b+d_b	
				150*	B
				80	
				r_b+d_b	

*reported for both type A and type B specimen configurations

Table 3-3(c) CFCC 1x7 7.5 mm diameter specimens

Material	Bend Radius r_b	Bend Radius r_b/d_e	l_d* (mm)	l_d (mm)	Stirrup Anchorage Type
CFCC	20	3.2	45	150	A
				80	
				r_b+d_b	
	30	4.8	22.5 (3DB)	150	A
				100	
				r_b+d_b	
			45	150	
				100	
				r_b+d_b	
			67.5	150	
				100	
				r_b+d_b	
			90	150	
				100	
				r_b+d_b	
			150 ($20d_b$)	150	
				100	
				r_b+d_b	
			---	150	B
				100	
				r_b+d_b	

Table 3-4 C-BAR specimens

Material	Bend Radius r_b	Bend Radius r_b/d_e	l_d* (mm)	l_d (mm)	Stirrup Anchorage Type	No. of specimens tested
C-BAR	50	4.00	72 ($6d_e$)	r_b+d_b	A	2
				250		2
			145 ($12\ d_e$)	150		2
				100		2
				r_b+d_b		6
			—	250	B	3
				150		1
				100		2
				r_b+d_b		10

Table 3-5 Steel specimens

Material	Nominal Diameter d_b (mm)	Bend Radius r_b	Bend Radius r_b/d_e	l_d* (mm)	l_d (mm)	Stirrup Anchorage Type	No. of specimens tested
Steel	6.35	20	3.00	40 ($6d_b$)	150	A	1
					80		1
					r_b+d_b		1
				—	150*	B	—
					r_b+d_b		1
	10	40	4.00	—	r_b+d_b	B	3

* reported for both type A and type B specimen configurations

3.3.2 Testing Set-up

The testing set-up shown in Figures 3-6 and 3-7 consisted of:

1) A 500 kN hydraulic jack, used to apply relative displacement between the concrete blocks.
2) A 75 kip (330 kN) donut loadcell used to measure the load and transmit data to the Data Acquisition system.
3) Steel plates and plaster bags used to distribute the applied load uniformly on each concrete block surface.
4) 300 mm PI gauges (electric strain gauges mounted to a metal arc that monitor the deflection of the arc as the two ends are moved), attached to each side of the specimen, to monitor the relative displacement of the blocks.
5) An elaborate protection system, constructed to avoid damage to the equipment, with rollers placed along the bottom of one block to reduce friction between the block and the testing bed.

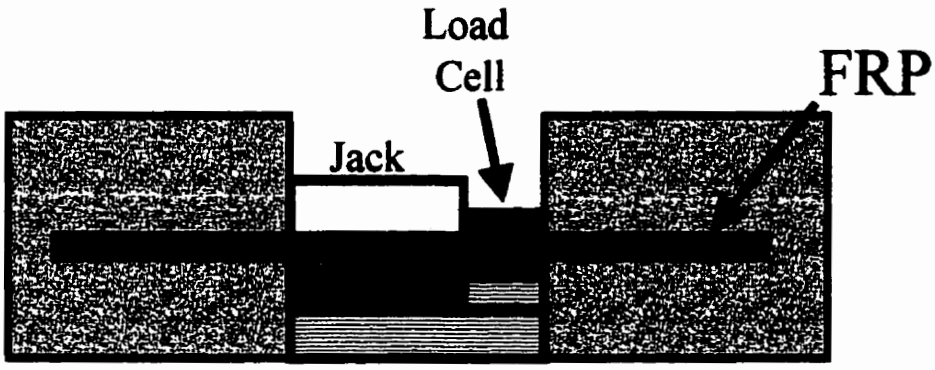

Figure 3-6 Bend test setup

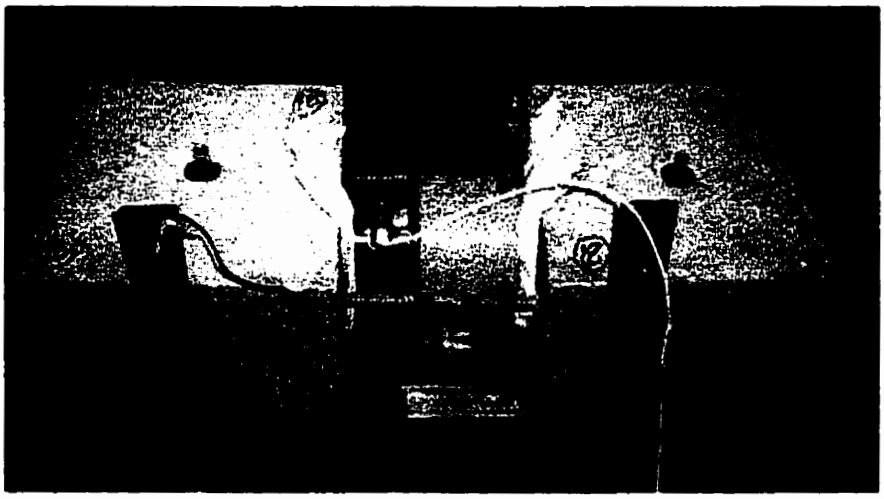

Figure 3-7 Bend test photograph

3.3.3 Instrumentation

The strain in the stirrup was measured in two ways. Electric strain gauges were bonded to one branch of the stirrup to measure strain. In addition, an MTS extensometer was attached to one branch of the stirrup in the clear span to measure strain.

The relative displacement between the two concrete blocks was also measured. PI gages (300 mm) were attached to each side of the specimen to continually record the movement of the specimen. The PI gauges were affixed at the level of the stirrup and the readings from these gauges were recorded by the data acquisition system

The load cell, MTS extensometer, PI gauges and strain gauges were all connected to the data acquisition system, which was configured to receive output signals every two seconds. The MTS extensometer was removed at roughly 80% of the predicted rupture load to avoid damage to the extensometer.

3.3.4 Test Procedure

The hydraulic jack and load cell were positioned at the level of the stirrup to avoid eccentricity during the application of load. Load was applied manually through a pump and

was increased at a constant rate. The load cell, extensometer, strain gauge, and PI gauge readings were monitored on the computer for the duration of the test while a file was being recorded for later analysis.

3.4 Phase II – Inclined Crack Effect

Due to the diagonal nature of shear cracks, these cracks intersect the stirrups at an angle and as the crack width is increased, the stirrups are subjected to transverse loading in addition to axial load. To determine the losses associated with the inclined crack effect the following parameters were examined:

Material type - CFRP Leadline, GFRP C-BAR, steel

Angle - 25°, 35°, 45°, 53°, 60°

3.4.1 Specimen Design & Fabrication

The specimen configuration is shown in Figure 3-8. The stirrups were placed as shown, at specified angles of 25, 35, 45, 53 or 60 degrees. Table 3-6 shows a summary of the different specimens. Steel reinforcement was placed in each end of the specimen to control cracks during testing. The steel cage was constructed using 10 mm deformed steel bars and 6 mm smooth steel bars. The specimen was pre-cracked at the center by the placement of sheet

metal between the two sides. A reduced concrete section measuring 75 x 235 mm was left in the center section (where the stirrups crossed) to allow for natural crack development and transfer of the load from the concrete to the stirrups. Two indentations were created on either side of the specimen at the center to allow room for a hydraulic jack and loadcell. These indentations were angled towards the center of the specimen to reduce the amount of unnecessary concrete in the specimen near the critical center crack area and to further control the specific crack location.

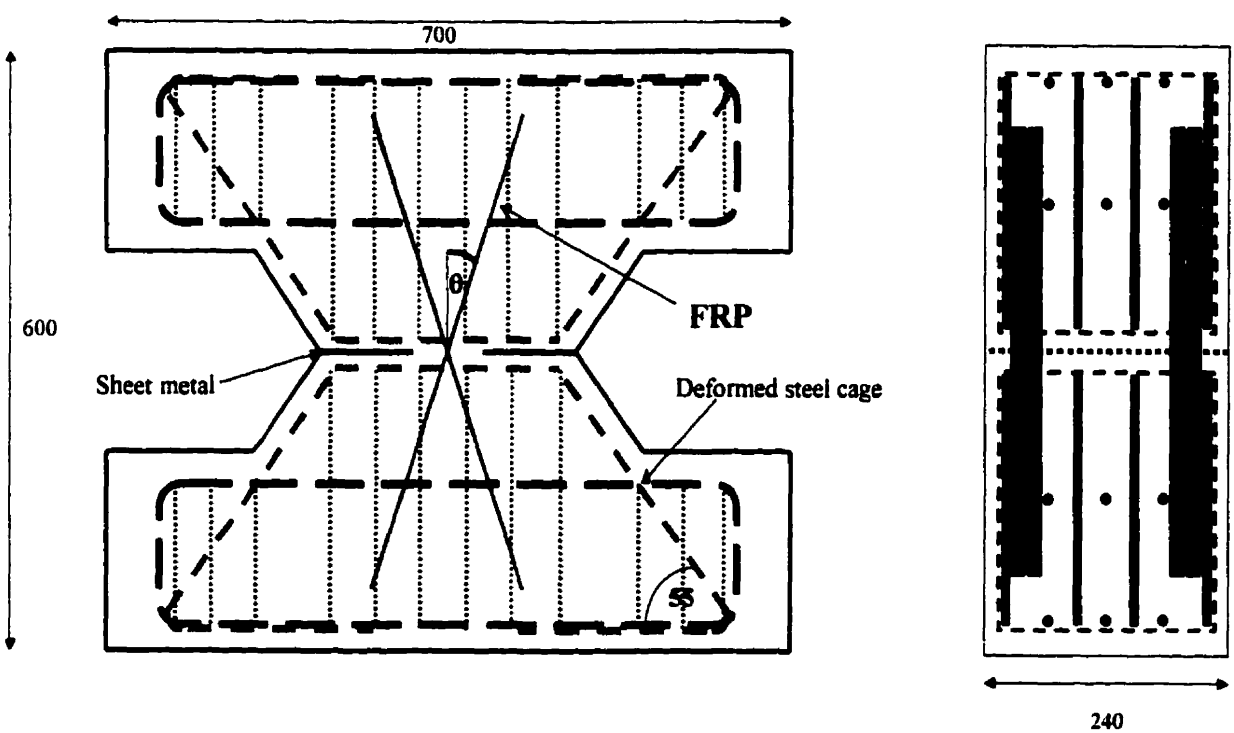

Figure 3-8 Inclined crack specimen configuration

Table 3-6 Inclined Crack Specimens

Material	Nominal Diameter d_b (mm)	Effective Diameter d_e (mm)	Stirrup Angle (deg)
Leadline	rect. 10x5 mm	7	25
			35
			45
			53
			60
C-BAR	12	12	25
			35
			45
			53
			60
Steel	6.35	6.35	30
			45

3.4.2 Test Set-up

A large plywood board was used as a testing surface with steel plates on one end and aluminum rollers on the other end to allow for the free relative movement. The equipment used in this test was similar to that used for the bend specimens:

1) 500 kN hydraulic jacks placed on either side of the specimen in the designated indentations to apply relative displacement between both ends.

2) A 75 kip (330 kN) Donut loadcell on each side to measure the applied load.

3) Steel plates and plaster bags placed against concrete load-bearing surfaces to uniformly distribute the applied load.

A typical test set up is shown in Figure 3-9.

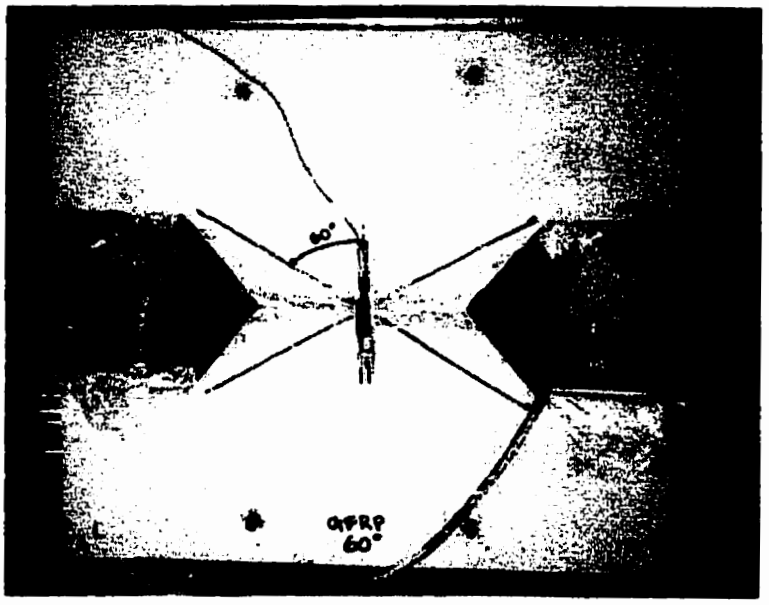

Figure 3-9 Inclined crack specimen test setup

3.4.3 Instrumentation

The instrumentation for these tests consisted of two parts. First, on the top and the bottom stirrup in the specimen, electrical strain gauges were attached at the crack location to monitor the strain in the stirrup when it became load bearing due to cracking of the concrete. Along the top of the specimen, a 100 mm PI gauge was attached to monitor crack width and to identify the initiation of load transfer from the concrete to the FRP stirrups.

3.4.4 Test Procedure

The hydraulic jacks were connected to independent pumps to allow full control over the load application on both sides. The load was applied at a constant rate from both pumps and continually monitored. If necessary, adjustments were made manually to the pumping rate to evenly load both sides. Load was applied until the failure of one of the stirrups occurred. All information gathered by the attached instruments was displayed and was simultaneously recorded by the data acquisition system. A photograph of the entire testing area, with a test in progress, is shown in Figure 3-10. The results of this group of tests are given in Chapter 4.

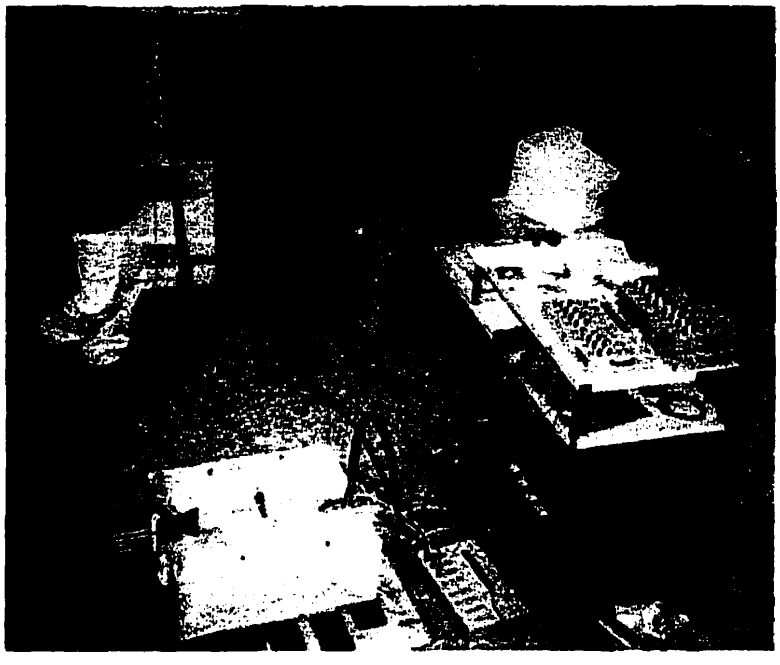

Figure 3-10 Inclined crack test photograph

CHAPTER 4: EXPERIMENTAL RESULTS AND DISCUSSION

4.1 General

A total of 113 specimens were fabricated and tested at the R.W. McQuade Structures Laboratory at the University of Manitoba to examine the behaviour and determine the strength of FRP stirrups as shear reinforcement for concrete structures. The testing program consisted of 101 specimens designed to investigate the bend effect, and 12 specimens tested to evaluate the effect of inclined cracks located at an angle to the stirrups. The parameters included in the bend effect study were the material, bend radius (r_b), bar diameter (d_e), embedment length (l_d), anchorage conditions, and tail length (l_d*). The inclined crack study included two parameters: the material type and the stirrup angle with respect to the crack. The results of both of these studies are presented and discussed in this chapter.

4.2 Phase I – Bend Capacity

The first phase of the experimental program was undertaken to evaluate the effect of the bend on the strength of FRP stirrups. A summary of the 101 specimens tested is shown in Tables 4-1, 4-2, 4-3, and 4-4. These tables indicate the parameters for each specimen, failure stresses and mode of failure. The symbols used for the different modes of failure in the tables are described as follows:

- R-S: Rupture of the FRP stirrups (or yielding of the steel stirrups) along the straight portion of the stirrup between the two concrete blocks
- R-B: Rupture of the FRP stirrups (or yielding of the steel stirrups) at the stirrup bend location
- R-D: Rupture of the stirrups at the end of the debonded length inside the concrete block
- S: Slippage of the bonded part of the stirrup
- S-RB: Slippage of the bonded part of the stirrup followed by rupture of the stirrup at the bend portion
- R-BD: Rupture of the fibres at both the bend and at the end of the debonded length

Table 4-1 Bend test results: Leadline

Material	Bend Radius r_b	r_b/d_e	l_d^* (mm)	l_d (mm)	Stirrup Anchorage Type	Failure stress f_{fv}	f_{fv}/f_{fuv}	Failure Mode
Leadline	20	3	21(3d_e)	r_b+d_b	A	632	0.35	S-RB
			42	150		1404	0.78	R-D
				r_b+d_b		639	0.36	S-R
			63	r_b+d_b		737	0.41	S-RB
			84	150		1168	0.65	R-B
				r_b+d_b		728	0.40	S-RB
			120	r_b+d_b		793	0.44	S-R
			---	150	B	1242	0.69	R-B
				100		1335	0.74	R-D
				r_b+d_b		715	0.40	R-B
	50	7	21 (3d_e)	150	A	1057	0.59	R-B
				r_b+d_b		797	0.44	R-B
			42	150		1235	0.69	R-B
				r_b+d_b		955	0.53	R-B
			63	150		1062	0.59	R-B
				r_b+d_b		813	0.45	R-B
			84	150		1053	0.58	R-B
				r_b+d_b		935	0.52	R-B
			120 (18d_e)	350		1763	0.98	R-S
				300		1504	0.84	R-B
				250		1638	0.91	R-S
				150		1149	0.64	R-B
				r_b+d_b		962	0.53	R-B
			---	150	B	1176	0.65	R-B
				100		987	0.55	R-B
				r_b+d_b		981	0.55	R-B
CFRP 1 straight	N/A	N/A	N/A	300	N/A	1106	0.61	S
				150		874	0.49	S

R-S: Rupture of stirrups along straight portion between concrete blocks
R-B: Rupture of stirrups at the bend
R-D: Rupture of stirrups at the end of the debonded length inside the concrete
S: Slippage of the bonded portion of the stirrup
S-RB: Slippage of bonded portion of stirrup followed by rupture at the bend
R-BD: Rupture of some fibres at the bend and others at the end of the debonded length

Table 4-2 (a) Bend test results: CFCC 5mm 7-wire

Material	Bend Radius r_b	Bend Radius r_b/d_e	l_d* (mm)	l_d (mm)	Stirrup Anchorage Type	Failure stress f_{fv}	f_{fv}/f_{fuv}	Failure Mode
CFCC 5mm (7-wire)	15	4.2	45 ($9d_b$)	150*	A	2145	1.2	R-S
				80		1975	1.11	R-S
				r_b+d_b		916	0.51	R-B
				150*	B	2145	1.2	R-S
				80		2156	1.21	R-S
				r_b+d_b		1455	0.82	R-B

*reported for both type A and type B specimen configurations

Table 4-2 (b) Bend test results: CFCC 5mm single wire

Material	Bend Radius r_b	Bend Radius r_b/d_e	l_d* (mm)	l_d (mm)	Stirrup Anchorage Type	Failure stress f_{fv}	f_{fv}/f_{fuv}	Failure Mode
CFCC 5mm (single)	15	3.4	45 ($9d_b$)	150*	A	1957	1.06	R-S
				80		1973	1.07	R-S
				r_b+d_b		983	0.53	R-B
				150*	B	1957	1.06	R-S
				80		1949	1.06	R-S
				r_b+d_b		1187	0.64	R-B

*reported for both type A and type B specimen configurations

Table 4-2 (c) Bend test results: CFCC 7.5mm 7-wire

Material	Bend Radius r_b	r_b/d_e	l_d^* (mm)	l_d (mm)	Stirrup Anchorage Type	Failure stress f_{fv}	f_{fv}/f_{fuv}	Failure Mode
CFCC 7.5mm (7-wire)	20	3.2	45	150	A	1900	1.01	R-B
				80		1421	0.76	R-B
				r_b+d_b		798	0.43	R-B
	30	4.8	22.5 ($3d_b$)	150	A	1590	0.85	S-RB
				100		1352	0.72	S-RB
				r_b+d_b		789	0.42	R-B
			45	150		1729	0.92	S-RB
				100		1641	0.88	S-RB
				r_b+d_b		1159	0.62	R-B
			67.5	150		1768	0.94	R-S
				100		1398	0.75	R-B
				r_b+d_b		1475	0.79	R-B
			90	150		1875	1.00	R-B
				100		1867	0.99	R-D
				r_b+d_b		1846	0.98	R-B
			150 ($20d_b$)	150		1942	1.04	R-S
				100		1987	1.06	R-S
				r_b+d_b		1902	1.01	R-B
			---	150	B	2068	1.10	R-S
				100		1669	0.89	R-S
				r_b+d_b		1798	0.96	R-B

Table 4-3 Bend test results: C-BAR

Material	Bend Radius r_b	r_b/d_e	l_d* (mm)	l_d (mm)	Stirrup Anchorage Type	No. of specimens tested	Failure stress f_{fv}	f_{fv}/f_{fuv}	Failure Mode
C-BAR	50	4.00	72 (6d_e)	r_b+d_b	A	2	442	0.62	R-B
							400	0.56	R-S
				250		2	556	0.78	R-S
							517	0.73	R-S
			145 (12 d_e)	150		2	424	0.59	R-S
							450	0.63	R-D
				100		2	447	0.63	R-S
							416	0.58	R-D
				r_b+d_b		6	345*	0.48	R-B
			—	250	B	3	409	0.57	R-D
							511	0.72	R-D
							301	0.42	R-D
				150		1	586	0.82	Splitting**
				100		2	561	0.79	R-BD
							500	0.7	R-D
				r_b+d_b		10	347*	0.49	R-B

* average value

** failure by splitting of the concrete block, subsequent specimens protected against this type of failure

Table 4-4 Bend test results: Steel

Material	Nominal Diameter d_b (mm)	Bend Radius r_b	r_b/d_e	l_d* (mm)	l_d (mm)	Stirrup Anchorage Type	No. of specimens tested	Failure stress f_{fv}	f_{fv}/f_{fuv}	Failure Mode
Steel	6.35	20	3.00	40 (6d_b)	150	A	1	770	1.28	R-S
					80		1	757	1.26	R-S
					r_b+d_b		1	593	0.99	R-B
				—	150*	B	—	770	1.28	R-S
					r_b+d_b		1	669	1.12	R-B
	10	40	4.00	—	r_b+d_b	B	3	555	1.26	R-B

* reported for both type A and type B specimen configurations

4.2.1 Leadline Stirrups

In most of the Leadline stirrup specimens, failure occurred in the bent portion of the stirrup. The failure was initiated through bond loss between the inner fibres and the outer resin coating of the bar. Figure 4-1 shows typical Leadline specimens after failure following the splitting of the concrete block to inspect the embedded stirrup. The highest measured strength in the stirrups (98% of the guaranteed 1760 MPa) was achieved through the use of a large embedment length of 350 mm or $50d_e$. For comparison, the measured tensile strength of straight bars tested at the University of Manitoba was 1730 MPa.

The experimental results indicated that the strength of the Leadline stirrups was affected by the embedment length within the concrete block as related to the bend radius. At the smallest embedment length of r_b+d_e, the capacity of the stirrups was limited to 35 percent and 44 percent of the guaranteed strength for r_b/d_e ratios of 3.0 and 7.0 respectively. The capacity for the maximum embedment lengths of 150 mm ($21.5d_e$) and 350 mm ($50d_e$) were 78 percent and 98 percent of the guaranteed strength for the same two ratios of 3.0 and 7.0 respectively. These results clearly show the dependence of high strength on sufficient embedment within the concrete.

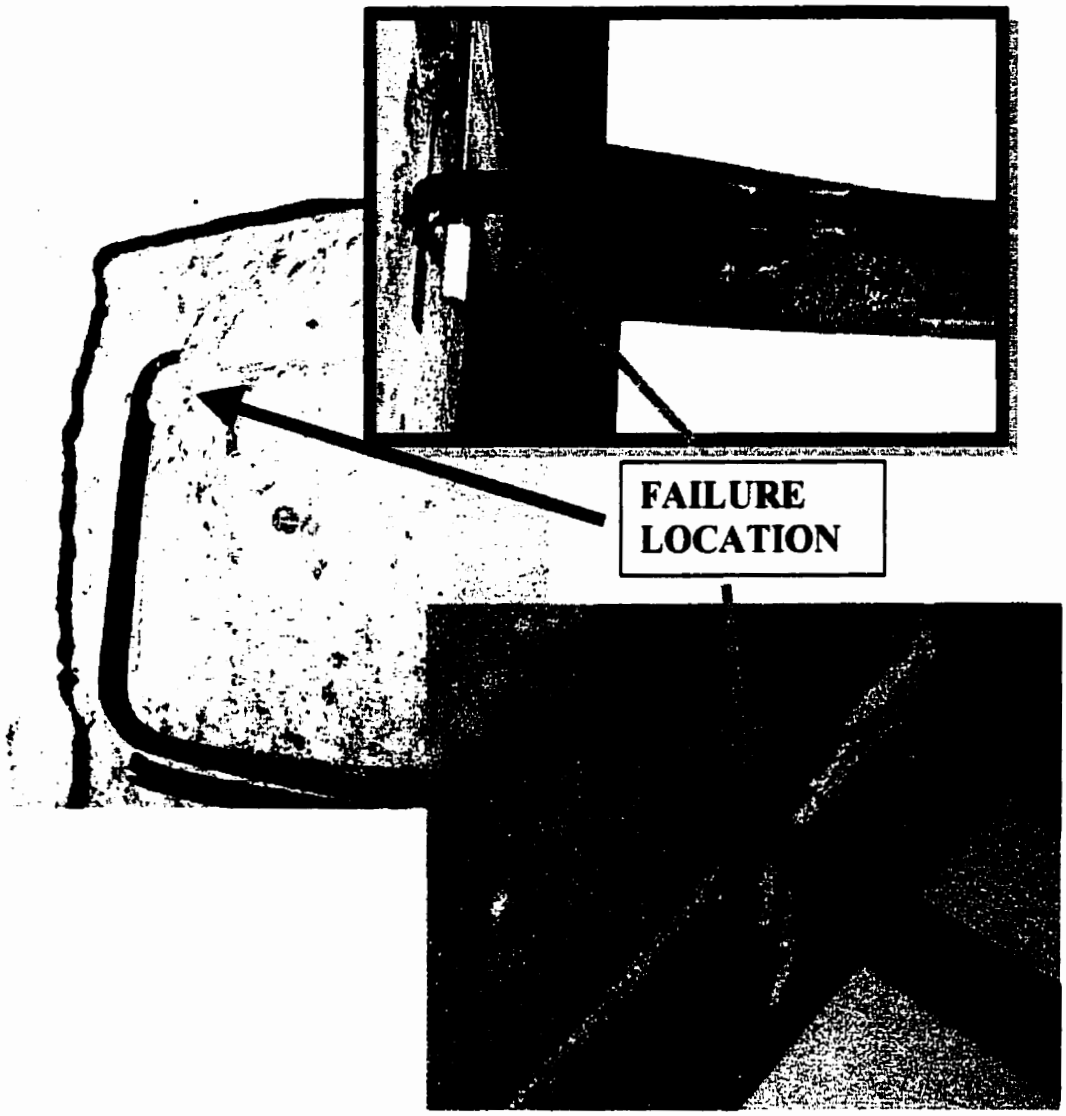

Figure 4-1 Failed Leadline bend specimens

Other factors affecting the capacity of these stirrups were the anchorage type and the tail length, l_d^*. For the Type A anchorage used for stirrups with a r_b/d_e ratio of 3.0, the stirrup capacity decreased as the tail length was decreased. However, the results also suggest that with a sufficient tail length in the Type A anchorage, the performance is similar to the Type B anchorage of the same stirrup. There was no significant variation in the stirrup capacity by varying the tail length for stirrups with a r_b/d_e ratio of 7.0

4.2.2 CFCC Stirrups

The Carbon Fibre Composite Cable, CFCC, stirrups exhibited significant losses due to the bend effect. As the embedment length was decreased, the measured ultimate strength was significantly lower than the guaranteed strength in the direction of the fibres. A maximum embedment length of 150 mm was sufficient to achieve the full capacity of the material in the direction of the fibres resulting in failure within the straight portion of the stirrup. Typical failures of the specimens, after splitting the concrete blocks following testing, are shown in Figure 4-2.

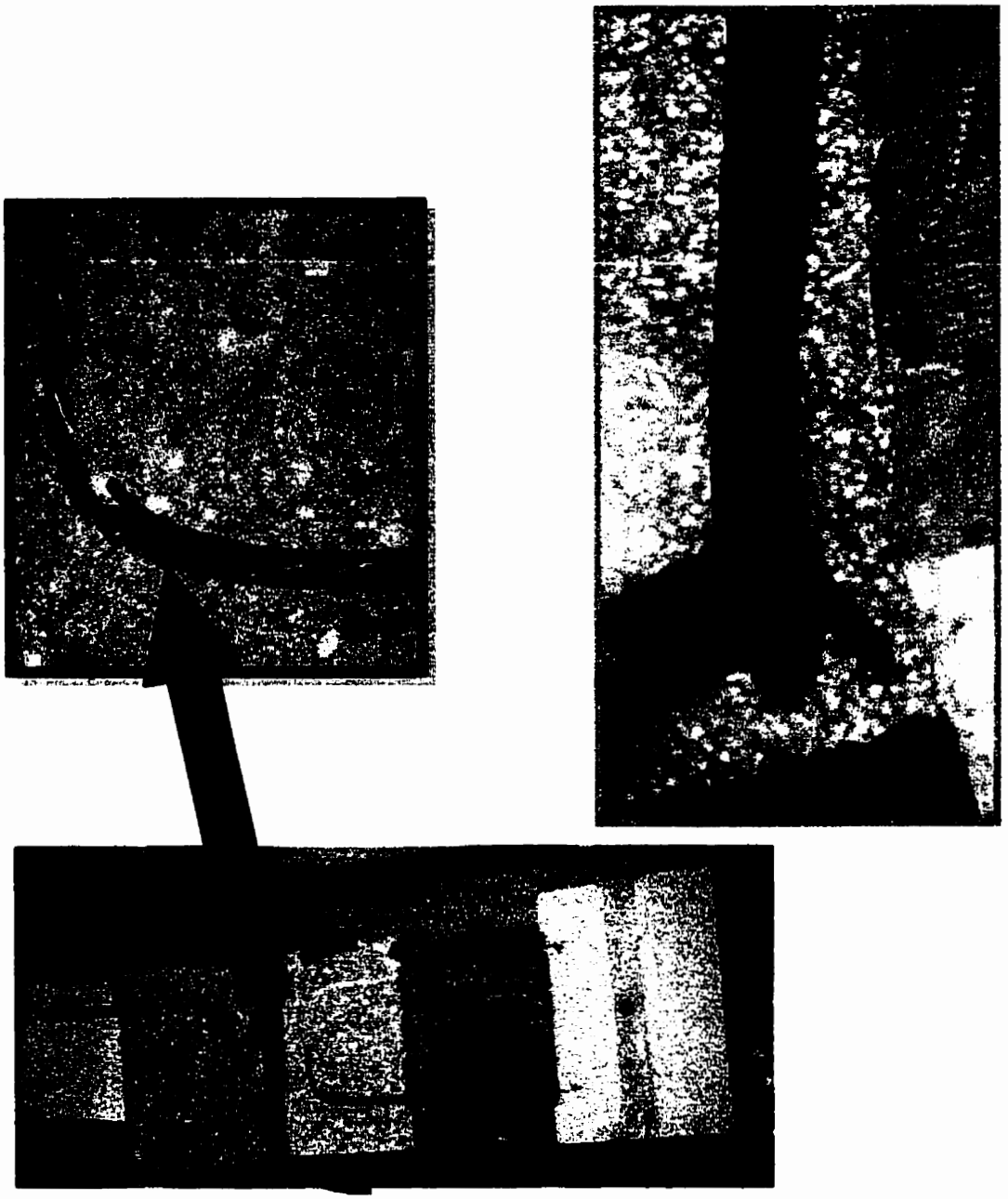

Figure 4-2 Failed CFCC bend specimens

For the smaller diameter specimens, stirrup strength ranged from 51 to 121 percent of the guaranteed strength in the direction of the fibres, with the variation due to changes in the embedment length. The strengths of the 5 mm 7-wire stirrups were ten percent higher

than the values for 7.5 mm 7-wire stirrups, with all other parameters equal. This difference may be attributed to shear lag across the cross section of the 7.5 mm stirrup. By examining the results of the 5 mm diameter stirrup tests it can be shown that an embedment length of only 80 mm ($16d_e$) is required to reach the guaranteed strength in the direction of the fibres.

The testing program for the 7.5 mm 7-wire stirrups included variation of all parameters. As the r_b/d_e ratio was increased, the measured capacity at the smallest embedment length of r_b+d_e ($5d_e$) was also increased. With a tail length of 45 mm ($7d_e$), the bend capacity was 43 and 62 percent of the strength in the direction of the fibres for r_b/d_e ratios of 3.2 and 4.8 respectively. These results clearly indicate that the bend radius greatly affects the bend capacity of CFCC stirrups.

The tail length, l_d^*, also affected the ultimate capacities for these stirrups. It can be seen in Table 4-2(c) that as the tail length is increased, the measured ultimate bend capacity increases. The capacity was 42 and 101 percent of the guaranteed strength in the direction of the fibres for tail lengths of 20 ($3d_e$) and 150 ($20d_e$) respectively. From these

results, using a tail length of 90 mm ($15d_e$), the differences between Type A and Type B anchorages are negligible. With a shorter tail length, the Type A anchorage specimens have a lower capacity than the Type B specimens. Beyond $15d_e$, the lapped end has sufficient length to be equivalent to a continuous anchorage.

4.2.3 C-BAR Stirrups

C-BAR stirrups exhibited less desirable behaviour due to premature material failure. At various locations along the stirrup, it was observed that the fibres were not parallel to the direction of the stirrup. This imperfection or "waving" of the fibres caused premature failure of the stirrups. Figure 4-3 shows photos of a typical C-BAR stirrup both before and after failure, where the waving effect is clearly shown. This imperfection subjects the fibres to non-axial stresses and therefore causes a significant reduction of the ultimate capacity of the bar at this location. This type of imperfection was found in most of the stirrups but the location of the imperfection and the severity of the fibre misalignment varied. Using this type of material lead to inconsistent results from the different parameters considered to evaluate the capacity of the stirrups.

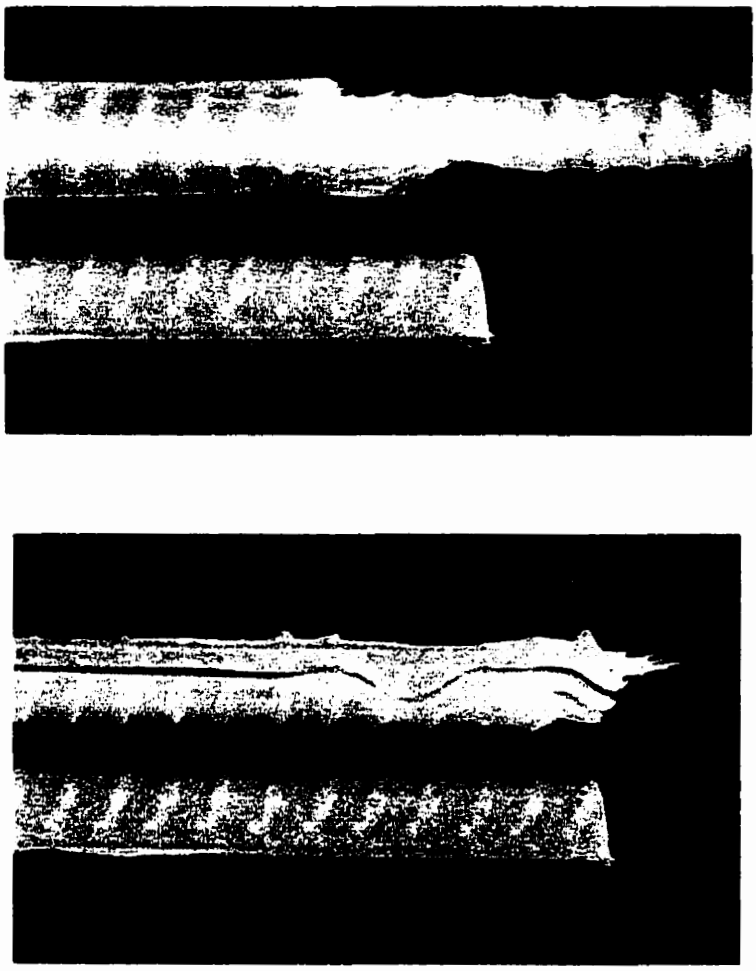

Figure 4-3 C-BAR "waving" imperfection

Despite the inconsistent results, the effect of a varied embedment length was clearly noted. When fully debonded, the stirrups had a capacity of 48 percent of the guaranteed value. In tension tests performed at the University of Manitoba, the measured tensile strength was only 640 MPa as compared to the guaranteed strength of 713 MPa provided by the manufacturer. The highest strength achieved in the bend specimens was only 82 percent of the guaranteed value. This loss of capacity from 82% to 48% shows the dependence of C-BAR stirrup strength on the embedment length. Unfortunately few other conclusions could be made due to the imperfections of the material used. A C-BAR stirrup with failure along the straight portion initiated by a defect is shown in Figure 4-4 while the failure of a C-BAR specimen at the bend can be seen in Figure 4-5.

Figure 4-4 C-BAR specimen failure along straight portion of stirrup due to defect

Figure 4-5 Failed C-BAR specimen at bend location

4.2.4 Steel Stirrups

The steel stirrup specimens failed due to yielding of the stirrups along the straight portion for specimens with a large embedment length, and yielding at the bend for specimens with the minimum embedment length. The failure stress in all specimens was equal to the guaranteed strength of a straight bar due to the isotropic behaviour of steel. While losses due to the bend effect were not noted and should not be present in this material, slippage could occur in specimens with short tail lengths.

4.3 Effect of Bend Radius on Bend Capacity

For most materials used in this program, test results indicated that the ultimate capacity was higher for the stirrups with the larger bend radius. This behaviour is a result of the inner fibres at the bend of small radius stirrups showing more severe bending and buckling in comparison to stirrups with a larger bend radius. Results showed that the variation of the bend radius had a more pronounced effect on CFCC specimens than Leadline specimens.

The relationship between the measured stress at failure to the guaranteed strength parallel to the fibres, f_{fv}/f_{fuv}, as affected by the bend radius to bar diameter ratio, r_b/d_e, is shown in Figure 4-6. Equations 4-1 and 4-2, recommended by the JSCE research committee (1997) giving the average values (of experimental data) and a conservative design equation, are shown on the same figure.

$$\frac{f_{fv}}{f_{fuv}} = 0.09\frac{r_b}{d_e} + 0.3 \leq 1.0 \qquad (4\text{-}1)$$

$$\frac{f_{fv}}{f_{fuv}} = 0.05\frac{r_b}{d_e} + 0.3 \leq 1.0 \qquad (4\text{-}2)$$

where,

f_{fuv} = ultimate strength of the FRP material in the direction of the fibres

r_b = bend radius

d_e = the effective bar diameter

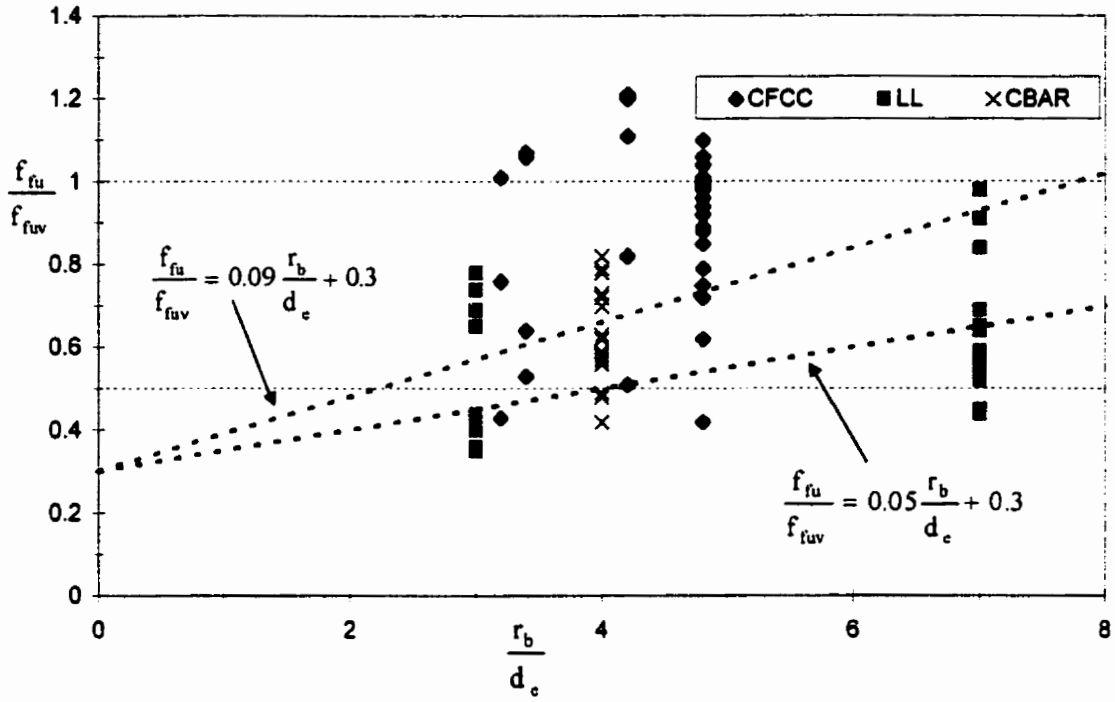

Figure 4-6 Effect of bend radius on stirrup capacity with equations proposed by JSCE (1997)

Figure 4-6 indicates that the JSCE equations are below the average of the measured data for CFCC and C-BAR stirrups tested in this program. However, the equation overestimates the strength for the Leadline stirrups with a large bend radius.

Test results were used to establish design recommendations for the bend radius of FRP stirrups. In order to achieve a stirrup capacity greater than 50 percent of the guaranteed

strength in the direction of the fibres a bend radius to bar diameter ratio r_b/d_e of 4.0 should be used for CFCC and C-BAR stirrups and 7.0 for the Leadline stirrups. Therefore, for the detailing of CFCC and C-BAR stirrups the bend radius r_b shall not be less than $4d_e$ or 50 mm, whichever is greater. For Leadline stirrups the bend radius r_b, shall not be less than $7d_e$ or 50 mm.

4.4 Effect of Embedment Length on Bend Capacity

Test results indicated that a reduction of the embedded length of the stirrup exposes the bend zone to much higher stresses causing a reduction in strength. If the embedment length is not sufficient to develop the full strength of the bar, losses will occur due to the reduced strength at the bend. The effect of the embedment length for CFCC, Leadline, and C-BAR stirrups is shown in Figures 4-7, 4-8, and 4-9 respectively. The relation is provided in terms of the measured capacity to the guaranteed strength parallel to the fibres f_{fv}/f_{fuv}, and the embedment length as a function of the effective diameter, l_d/d_e.

The results show that the reduction in the strength occurs below a certain value of the l_d/d_e ratio for each type of stirrup. The l_d/d_e value was 20 for the CFCC Type A stirrups and 16 for CFCC Type B stirrups. Using the value of l_d/d_e of 5.0 representing the end of the bend zone, the measured average strength for CFCC stirrups using Types A and B

stirrups were 50 and 74 percent of the strength in the direction of the fibres, respectively, as shown in Figure 4-7. Figure 4-8 indicates that the limiting value of l_d/d_e for the Leadline stirrups to achieve the guaranteed strength f_{fuv} parallel to the direction of the fibres is 42. Using a small development length reduces the strength to 40 percent of the guaranteed strength parallel to the fibres, as shown in Figure 4-8. Equations 4-3, 4-4, and 4-5 given in the two figures can be used to predict the strength capacity of the stirrup f_{fv} for intermediate development lengths:

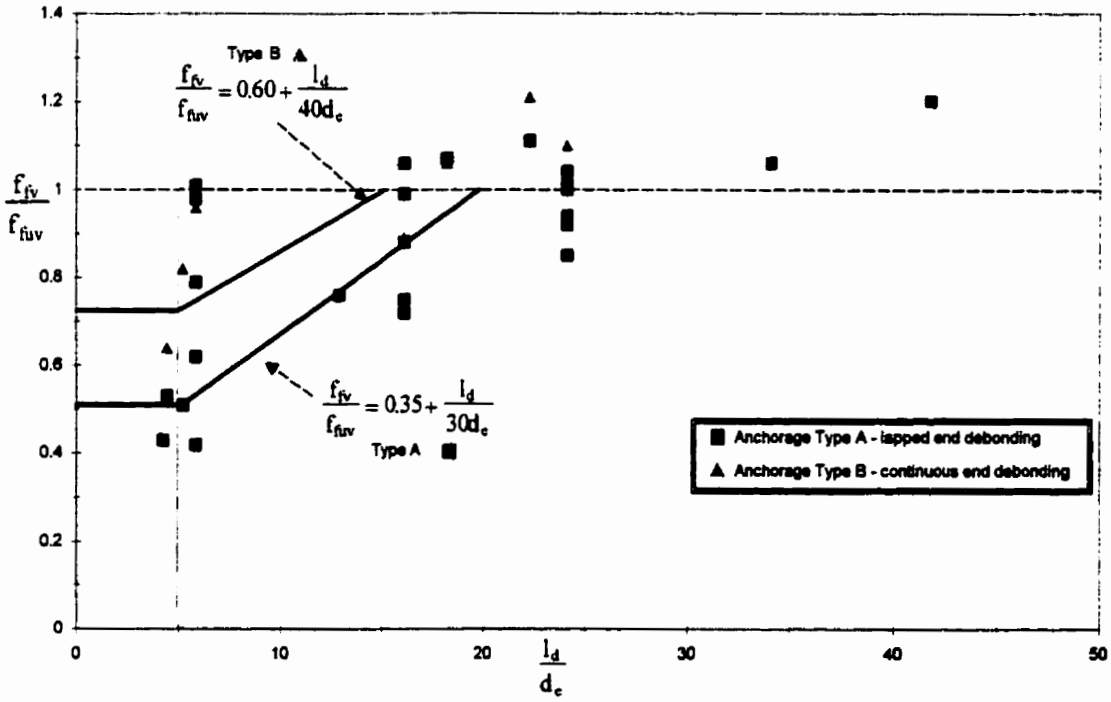

Figure 4-7 Effect of embedment length, l_d, on CFCC stirrup capacity

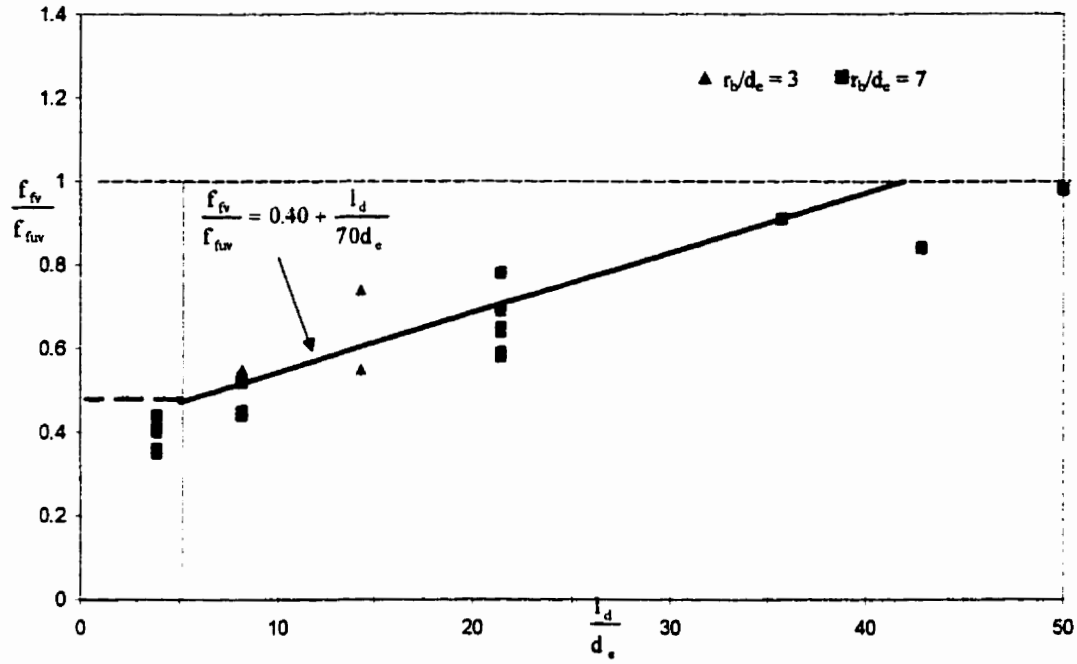

Figure 4-8 Effect of embedment length, l_d, on Leadline stirrup capacity

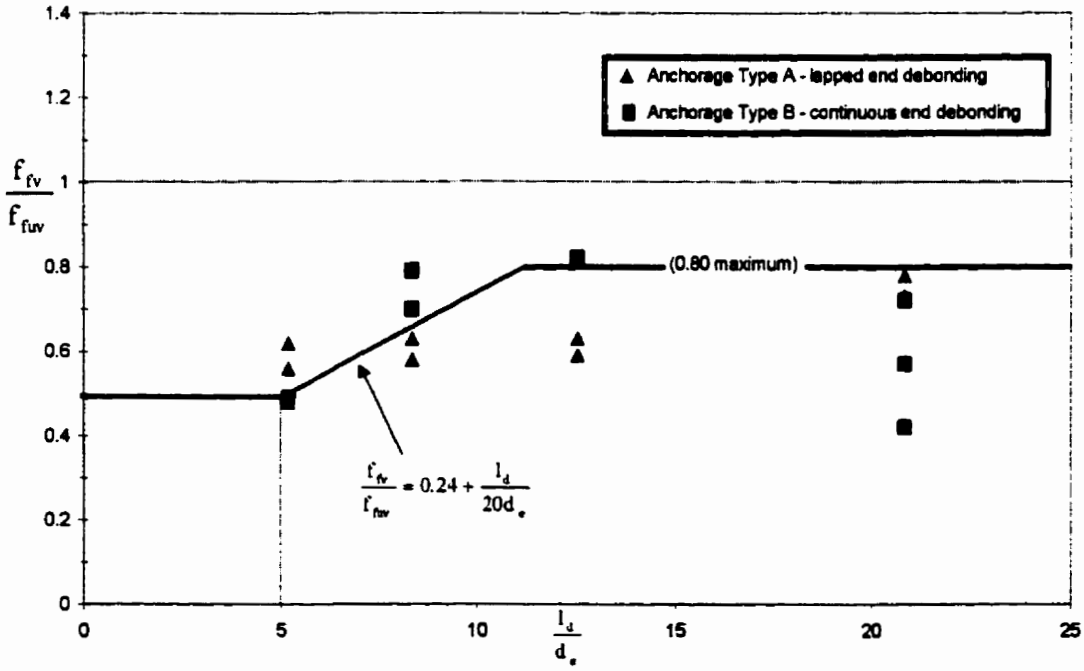

Figure 4-9 Effect of embedment length, l_d, on C-BAR stirrup capacity

CFRP CFCC

$$0.52 \leq \frac{f_{fv}}{f_{fuv}} = 0.35 + \frac{l_d}{30d_e} \leq 1.00 \qquad \text{Type A Anchorage} \qquad (4\text{-}3)$$

$$0.73 \leq \frac{f_{fv}}{f_{fuv}} = 0.60 + \frac{l_d}{40d_e} \leq 1.00 \qquad \text{Type B Anchorage} \qquad (4\text{-}4)$$

CFRP Leadline

$$0.47 \leq \frac{f_{fv}}{f_{fuv}} = 0.40 + \frac{l_d}{70d_e} \leq 1.00 \qquad (4\text{-}5)$$

The same analysis was attempted to predict the behaviour of the C-BAR stirrups. However, due to the "waving" effect from the imperfections introduced in the production of the bars, none of the specimens reached the full guaranteed strength in the direction of the fibres. The strength of C-BAR specimens reached only 80 percent of the strength in the direction of the fibres as shown in Figure 4-9. Due to this constraint, the failure criterion proposed based on test results is valid up to a maximum of 80 percent as given in equation 4-6.

GFRP C-BAR

$$0.49 \leq \frac{f_{fv}}{f_{fuv}} = 0.24 + \frac{l_d}{20d_e} \leq 0.80 \qquad (4\text{-}6)$$

4.5 Effect of Stirrup Anchorage on Bend Capacity

Two anchorage conditions were simulated in the experimental program. Type A stirrups simulate a standard hook anchorage, typically located in the compression zone of a reinforced concrete beam. Type B stirrups simulate a continuous anchorage typically located in the tension zone of the beam. It was observed that the tail length, l_d*, beyond the bend location for Type A specimens greatly influenced the strength of the anchorage.

Test results indicate that the capacity of the Type A anchorage is less than the Type B anchorage up to a transition value of the tail length (which is dependent on the bar type and diameter). This reduction in capacity is due to slipping at the bend for stirrups with a short tail length leading to higher stresses at the bend. For the 5 mm diameter CFCC specimens using only one l_d* length of 45 mm ($9d_e$), the Type A anchorage is notably weaker in comparison to the Type B anchorage. For the 7.5 mm diameter CFCC specimens, as l_d* reached $12d_e$, the strength of the Type A anchorage was equivalent to

the strength of the Type B anchorage. For l_d* less than $12d_e$, the strength of the Type A anchorage was less than for the Type B anchorage

For the two bend radii used, in the Leadline specimens, the Type B anchorage had a higher capacity than Type A until the tail length reached a value of $18d_e$. Therefore it can be concluded that the Type B, or continuous anchorage, has a greater capacity than the Type A, standard hook, anchorage unless a sufficient tail length, l_d*, of $12d_e$ for CFCC, and $18d_e$ for Leadline, is provided.

4.6 Effect of Tail Length on Bend Capacity

Based on the results obtained with the two anchorage types, the tail length l_d*, was varied in relation to the bar diameter in this investigation. In general, it was noted that as the tail length decreased, the ultimate capacity of the stirrups also decreased, due to a loss of anchorage. Without sufficient end anchorage, the bond along the embedment length becomes the only parameter affecting the capacity of the stirrup.

For the CFCC stirrups with 7.5 mm diameter, tail lengths of 3, 6, 9, 12, and 20 d_e were tested. Figure 4-10 indicates that as the tail length increases, the capacity as represented by the ratio f_{fv}/f_{fuv}, also increases. At a tail length of 15 d_e, the guaranteed stress value

was achieved for all embedment lengths. Below a tail length of 15 d_e the strength is lower than guaranteed to a minimum of 42 percent of the guaranteed strength in the direction of the fibres at a tail length of $3d_e$. Using the minimum embedment length of r_b+d_e, equation 4-7 is proposed to predict the capacity of the stirrup as a function of the tail length as follows:

CFCC

$$\frac{f_{fv}}{f_{fuv}} = 0.24 + \frac{l_d^*}{17d_e} \leq 1.00 \qquad (4\text{-}7)$$

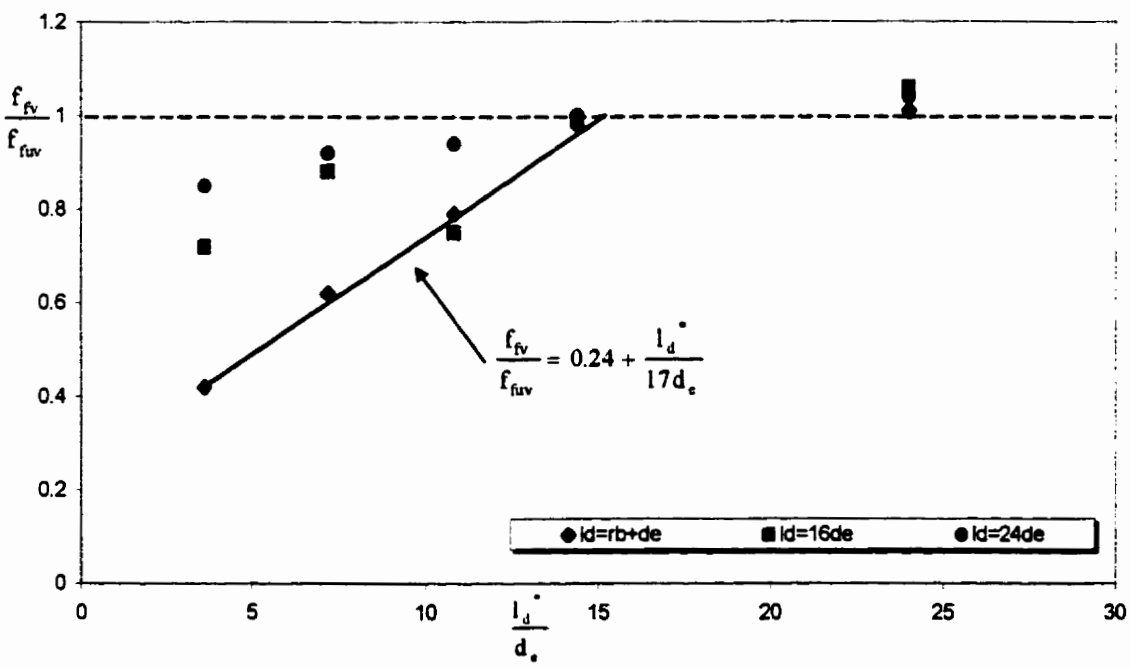

Figure 4-10 Effect of tail length, l_d*, on CFCC stirrup capacity

The observed relationship between f_{fv}/f_{fuv} and l_d^*/d_e was not as well-defined for Leadline specimens. The tail lengths of Leadline specimens were varied at 3, 6, 9, 12, and $18d_e$. For the small bend radius to diameter ratio, r_b/d_e of 3.0, behaviour was similar to what was observed for the CFCC specimens. However the strength was much lower, ranging from 35 to 44 percent of the guaranteed strength in the direction of the fibres. The capacity of stirrups with a larger bend radius to diameter ratio, r_b/d_e of 7.0 ranged from 44 to 53 percent of the guaranteed strength in the direction of the fibres. A minimum tail length of 70 mm ($10d_e$) is recommended to develop bend capacities of 40 and 50 percent of the guaranteed strength in the direction of the fibres for r_b/d_e ratios of 3.0 and 7.0 respectively.

Due to the material imperfections in the C-BAR stirrups, results from the study of tail length are inconclusive. Two tail lengths were used of $6d_e$, and $12d_e$. It was observed that the variation of tail length did not significantly affect the strength of the FRP stirrups. In general, for the detailing of all FRP stirrups, the tail length, l_d^*, shall not be less than $6d_e$ or 70 mm, whichever is greater.

4.7 PHASE II – Capacity at Inclined Crack

The second phase of the experimental program was undertaken to evaluate the effect of crack inclination on the capacity of FRP stirrups. A plot of the applied load versus the crack opening displacement based on PI gauge readings during a typical test for Leadline an angle of 35 degrees is shown in Figure 4-11(a). A plot showing the load versus the measured stirrup strain from the same test is shown in Figure 4-11(b). Both figures show the transfer of load from the concrete to the stirrups as the concrete cracks across the section. This behaviour simulates the load-transfer mechanism in concrete beams. Failed C-BAR and Leadline stirrups at the crack location after failure are shown in Figures 4-12 and 4-13 respectively.

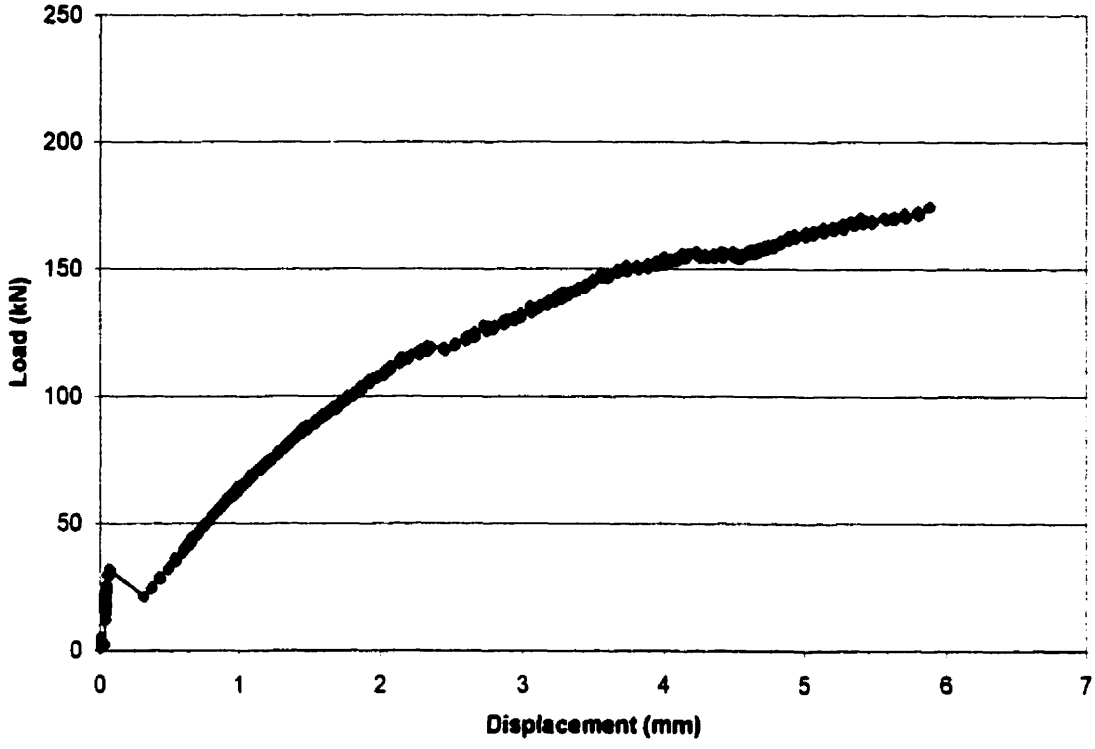

Figure 4-11 (a) Typical test plot of Load vs. PI gauge readings (Leadline - 35°)

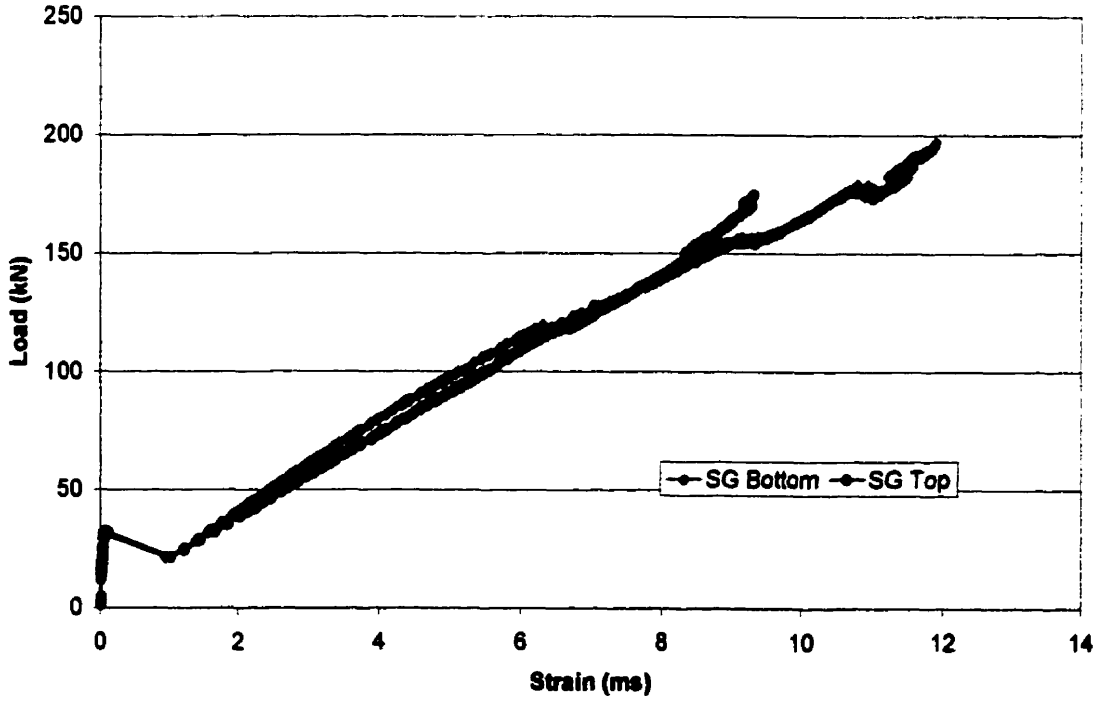

Figure 4-11 (b) Typical test plot of Load vs. strain gauges (Leadline - 35°)

Figure 4-12 Failed C-BAR stirrups

Figure 4-13 Failed Leadline stirrups

4.7.1 Test Results

A summary of the measured loads at failure for the inclined crack specimens is given in Table 4-5. This table also shows the material type, crack angle, failure stress, the ratio of failure stress to guaranteed failure strength in the direction of the fibres as well as the failure strain and the ratio between the measured and the guaranteed failure strain. In general, the PI gauge readings showed that the crack width at failure was progressively greater as the stirrup angle was increased. Figures 4-14 and 4-15, for Leadline and C-BAR respectively, show that the displacement for a given load is generally greater for stirrups at a greater angle due to deformation caused by a higher ratio of transverse to axial load. Models for the load-transfer mechanism are discussed in the following section.

Table 4-5 Inclined crack specimen test results

Material	Angle *	Failure Load (kN)	Failure Stress (MPa)	f_{fv}/f_{fuv}	Failure Stress (MPa)	f_{fv}/f_{fuv}	Failure Strain %	$\varepsilon_{fv}/\varepsilon_{fuv}$
			Bonded Model		Truss Model			
C-BAR	0*	322.28	713.00	1.00	713	1.00	1.74	1.00
	25	187.89	415.68	0.58	463	0.65	1.40	0.81
	35	186.97	413.65	0.58	505	0.71	1.61	0.93
	45	149.42	330.58	0.46	468	0.66	1.39	0.80
	50	174.65	386.40	0.54	641	0.90	1.44	0.83
	60	150.08	332.03	0.47	664	0.93	---	
	90*	77.35	171.12	0.24	---		---	
Leadline	0*	271.36	1763.00	0.98	1800	1.00	1.31	1.00
	25	195.19	1268.14	0.70	1398	0.78	0.96	0.73
	35	197.05	1280.24	0.71	1563	0.87	1.13	0.86
	45	159.42	1035.71	0.58	1461	0.81	1.02	0.78
	53	144.99	941.98	0.52	1565	0.87	1.20	0.92
	60	129.08	838.61	0.47	1676	0.93	---	
	90*	36.02	234.00	0.13	---		---	
Steel **	0*	83.60	660.00	1.00	660	1.00	---	
	30	65.87	520.00	0.79	600	0.91	---	
	45	59.54	470.00	0.71	665	1.00	---	
	90*	48.26	381.00	0.58	---		---	

*- from previous experiments: value of 0 from tension test and 90 degrees from dowel test

**- steel loads are at yielding

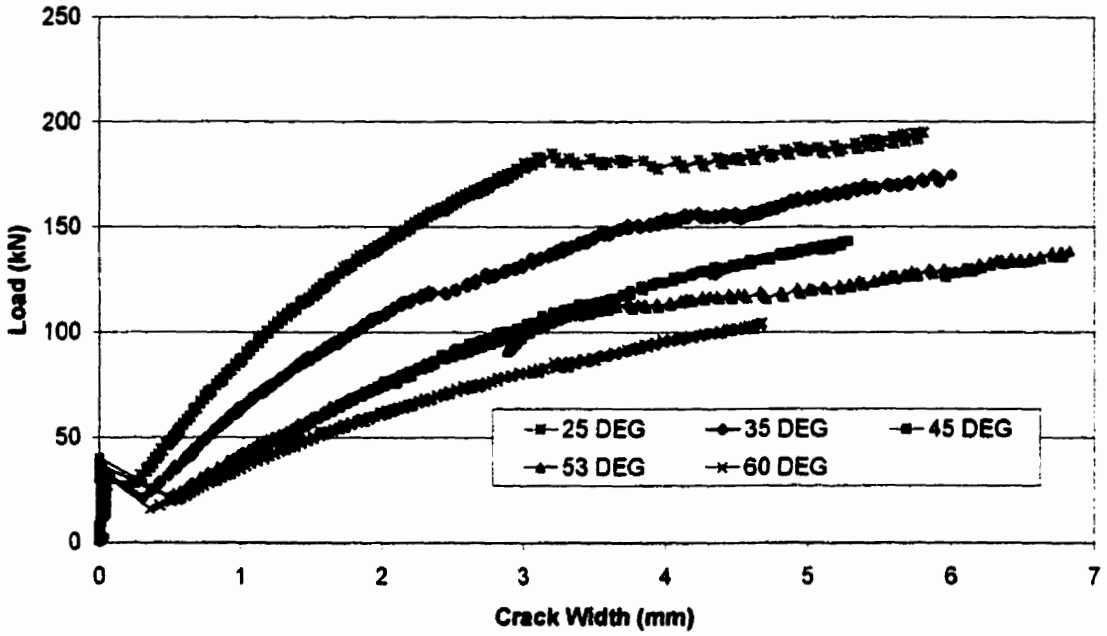

Figure 4-14 Load vs. Crack Width for Leadline

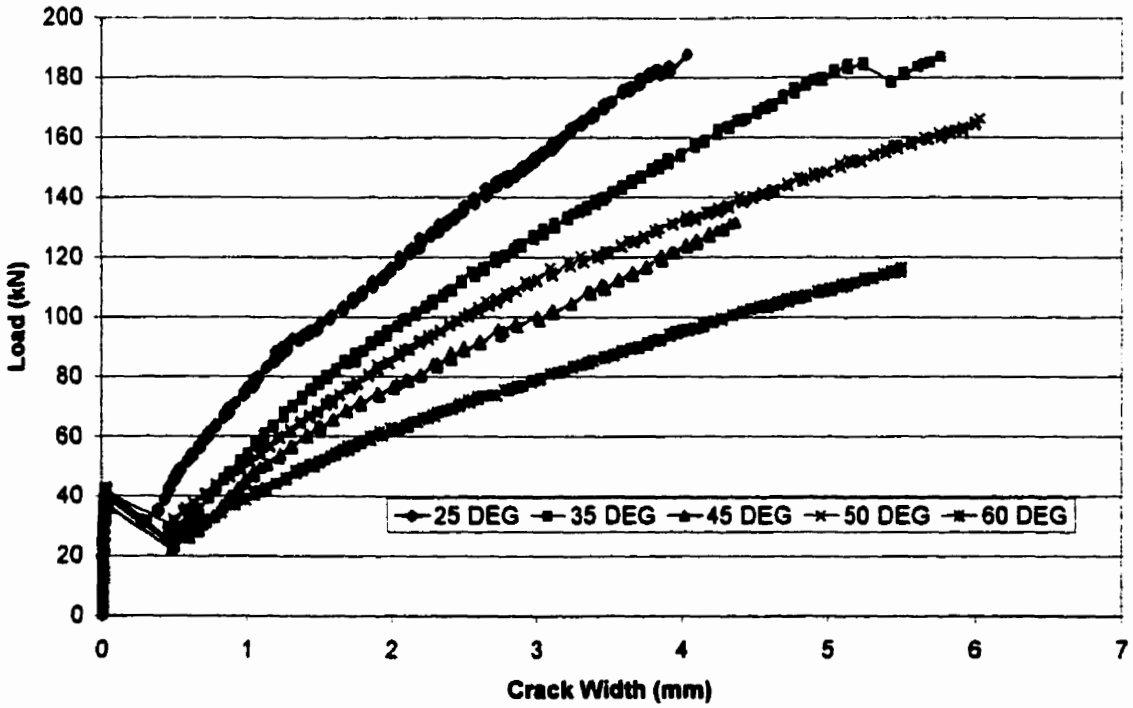

Figure 4-15 Load vs. Crack Width for C-BAR

4.7.2 Analysis of the Results

For the determination of the stirrup stresses the "bonded" model and the "truss" model are proposed to describe the load transfer mechanism as shown in Figure 4-16. The first model assumes that the stirrups are fully bonded within the concrete and therefore are restrained from deformation. The force equilibrium must be satisfied with both axial and shear forces within the stirrup cross-section and a resultant equal to half of the applied load. The stress is calculated using this resultant load divided by the cross-sectional area of the bar.

The second proposed mechanism models the load transfer similar to a truss mechanism. Due to concrete crushing a long debonded length occurs starting at the face of the specimen. With a rigid arm and a "pinned" connection at the end of this debonded length, the stirrup is allowed to deform and is not subject to shear force. The stress can be calculated using the tension force in the direction of the stirrup divided by the area of the stirrup.

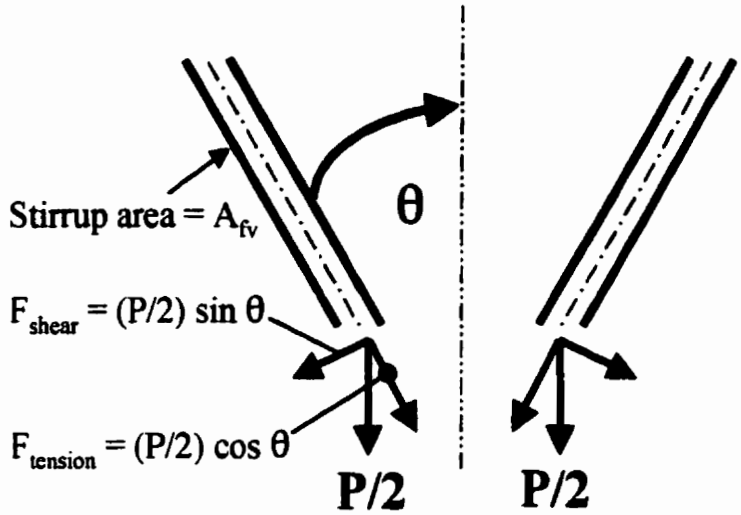

Stirrup stress: $f_{fv} = (P/2)/A_{fv}$

Figure 4-16 (a): Load Transfer Mechanism for the "Bonded" Model

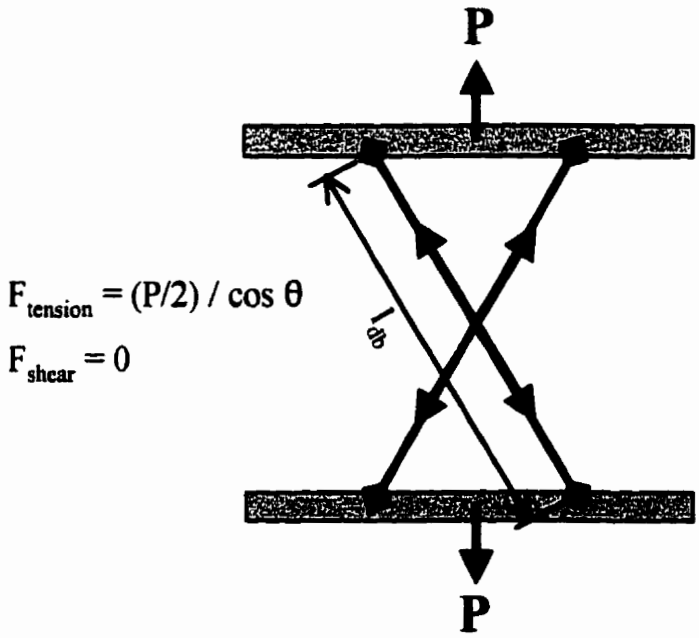

Stirrup stress: $f_{fv} = F_{tension}/A_{fv}$

Figure 4-16 (b): Load Transfer Mechanism for the "Truss" Model

4.7.2.1 "Bonded" Model

4.7.2.1.1 Steel Specimens

The results of the control specimens using steel stirrups agree with the Von Mises criterion for steel behaviour, as shown in Figure 4-17 and given in equation 4-8:

$$f^2_{tension} + 3f^2_{shear} = f^2_y \qquad (4\text{-}8)$$

where,

$f_{tension}$ = applied tensile strength equal to $f_{fv}\cos\theta$

f_{shear} = applied shear stress equal to $f_{fv}\sin\theta$

f_y = yield strength

Equation 4-8 can be expressed in terms of f_{fv}/f_{fuv} for direct comparison with the specimens used in this experimental program as given in equation 4-9.

$$\frac{f_{fv}}{f_{fuv}} = \sqrt{\frac{1}{\cos^2\theta + 3\sin^2\theta}} \qquad (4\text{-}9)$$

All of the measured values agree with this prediction as shown in Figure 4-17 including the lowest value of 58 percent of the yield strength at 90 degrees.

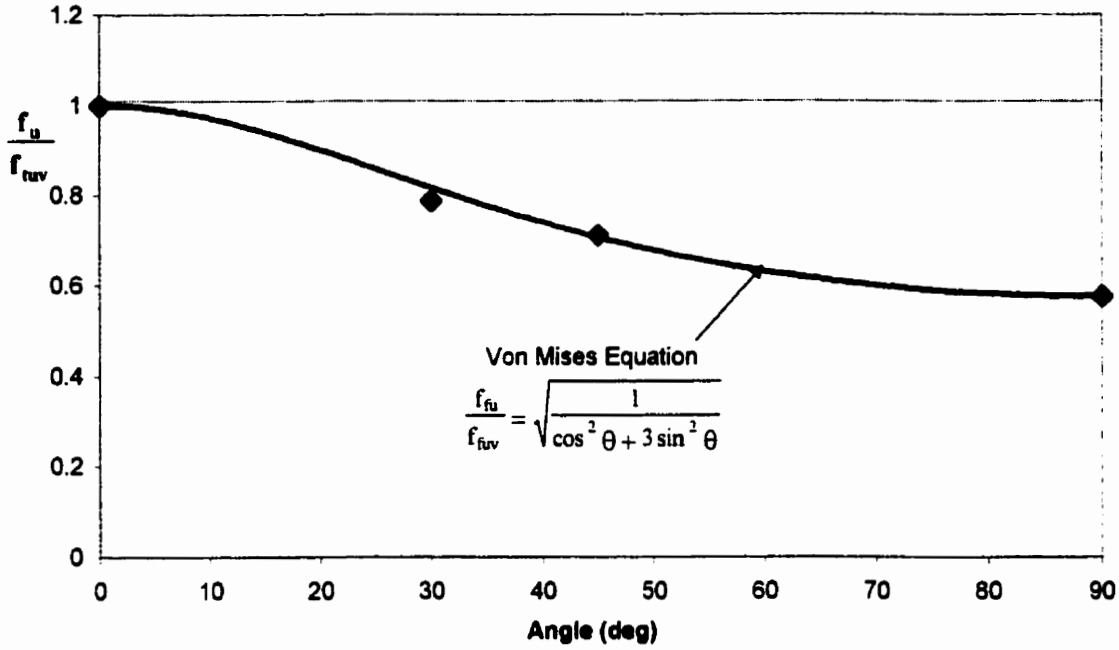

Figure 4-17 Effect of inclined crack on steel stirrup capacity

4.7.2.1.2 FRP Specimens

At an angle of zero degrees, the test becomes equivalent to that of the fully bonded bend specimens tested in Phase 1, where the guaranteed strength of the stirrups was achieved. Direct shear tests of the FRP bars correspond to a 90-degree crack angle and provide the lowest strength. Angles between these boundaries were tested using the inclined crack specimens. Test results of Leadline and C-BAR specimens described in this phase are

shown in Figures 4-18 and 4-19. Predictions by Maruyama et al. (1989) and Nakamura and Higai (1995) are shown on the same figures. Maruyama's equation for the prediction of stirrup capacity is valid for angles up to 30 degrees but is shown with an extension to f_{fv}/f_{fuv} equal to zero. In comparison to the measured values, this equation is extremely conservative in the prediction of strengths for the Leadline stirrups and slightly more accurate for the prediction of the C-BAR stirrup strengths. Nakamura and Higai's analytical equation is valid to 90 degrees but in comparison to measured values, is not accurate, especially for high angle specimens. The use of this equation results in zero strength for an angle of 90 degrees, however, both C-BAR and Leadline stirrups have a strength greater than zero for an angle of 90 degrees.

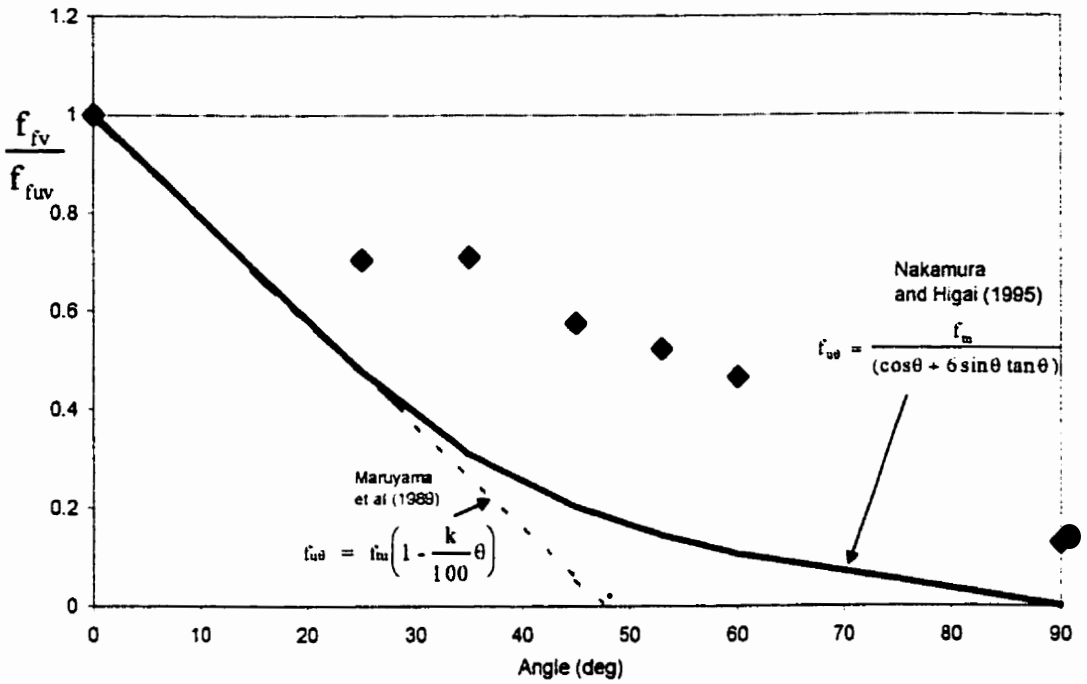

Figure 4-18 Effect of inclined crack on Leadline stirrup capacity

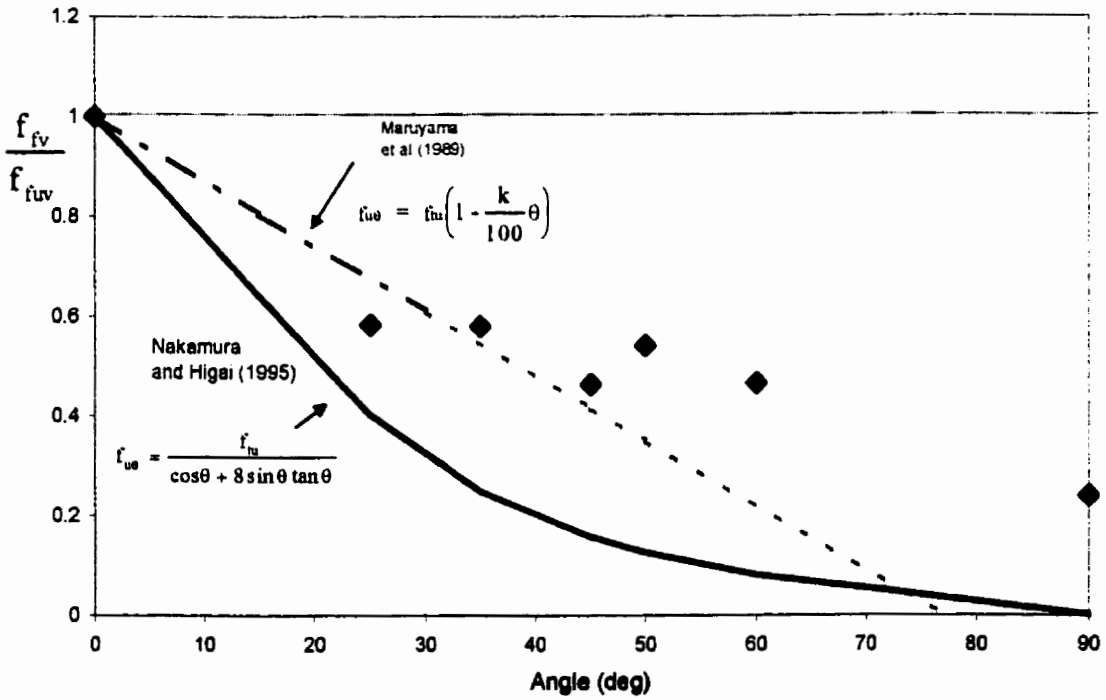

Figure 4-19 Effect of inclined crack on C-BAR stirrup capacity

Based on the test results obtained from this phase, equation 4-10 is a best-fit curve for the data as shown in Figure 4-20. This equation follows the format used by the Von Mises criterion for steel behaviour. Equation 4-10 accurately predicts the strengths of the stirrups for all the angles used in this investigation except for the strength at an angle of 90 degrees. However, since the 90-degree angle is not the focus of this study, the equation can be considered adequate for these specimens up to an angle of 60 degrees.

$$\frac{f_{fv}}{f_{fuv}} = \sqrt{\frac{1}{\cos^2\theta + 6\sin^2\theta}} \qquad (4\text{-}10)$$

For design purposes, equation 4-11 is proposed to provide more conservative values as shown in Figure 4-20.

$$\frac{f_{fv}}{f_{fuv}} = \sqrt{\frac{1}{\cos^2\theta + 12\sin^2\theta}} \qquad (4\text{-}11)$$

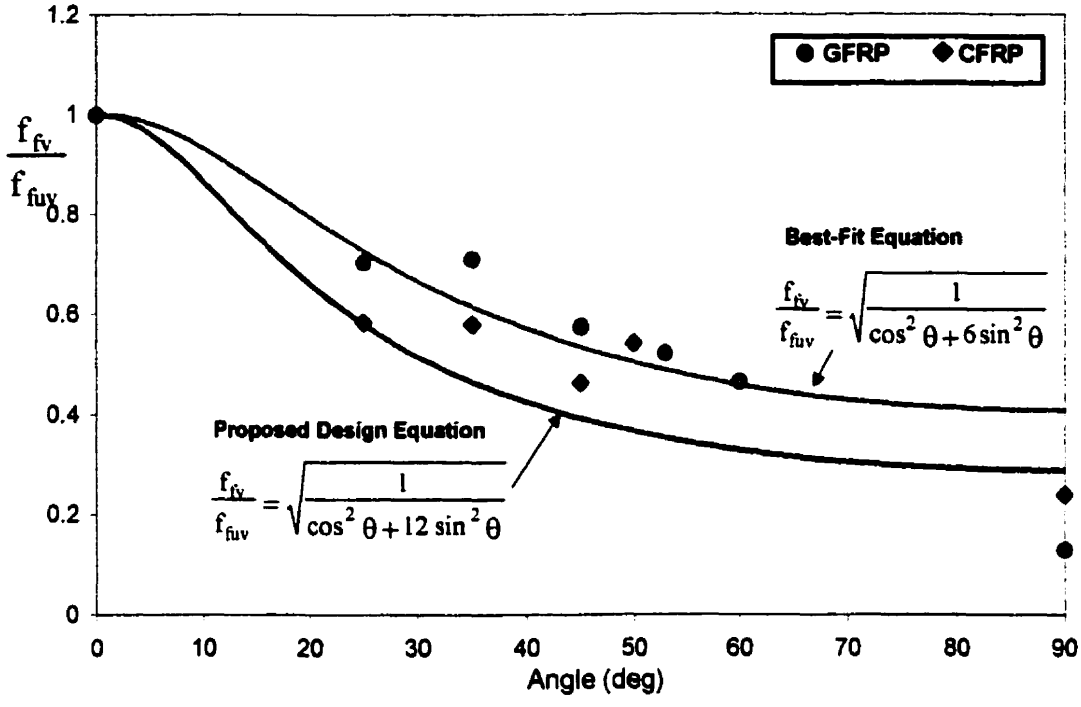

Figure 4-20 Proposed equations for FRP material

The measured ultimate strain in the stirrups at failure is shown in Figure 4-21. It can be seen that the ultimate strain is achieved in most of the specimens with C-BAR specimens whereas the strain in the Leadline specimens ranged from 74 to 91 percent of the ultimate value. The average strain at failure is approximately 83 percent of the strain parallel to the fibres as shown in Figure 4-21. These results indicate that the stirrup strain at failure is independent of crack orientation.

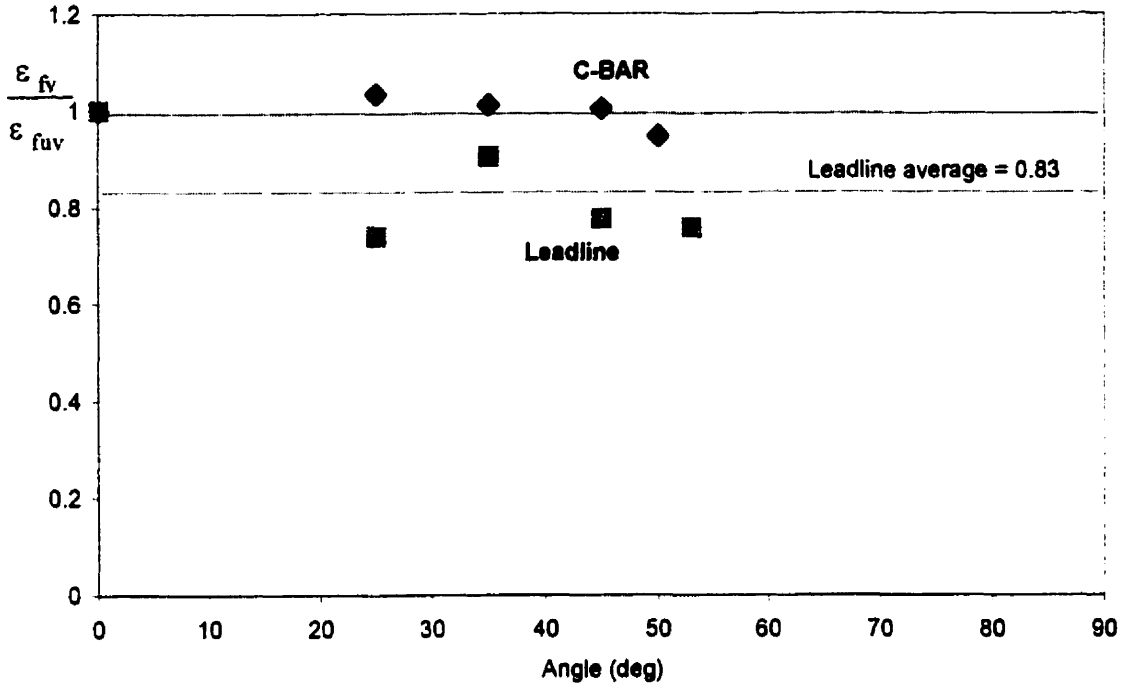

Figure 4-21 Measured ultimate strain in Leadline and C-BAR specimens

4.7.2.2 "Truss" Model

This model for the distribution of stresses assumes that the bond is lost between the stirrup and the concrete over a long length. This system performs as a truss with no shear force acting on the stirrup. Using this model, there is no obvious relationship between the angle and the stirrup stress for both the CFRP and GFRP stirrups as shown in Figure 4-22. As given in Table 4-5 and shown in Figure 4-22, the average f_{fv}/f_{fuv} ratio is 0.810, which corresponds with the average strain ratio from the FRP specimens.

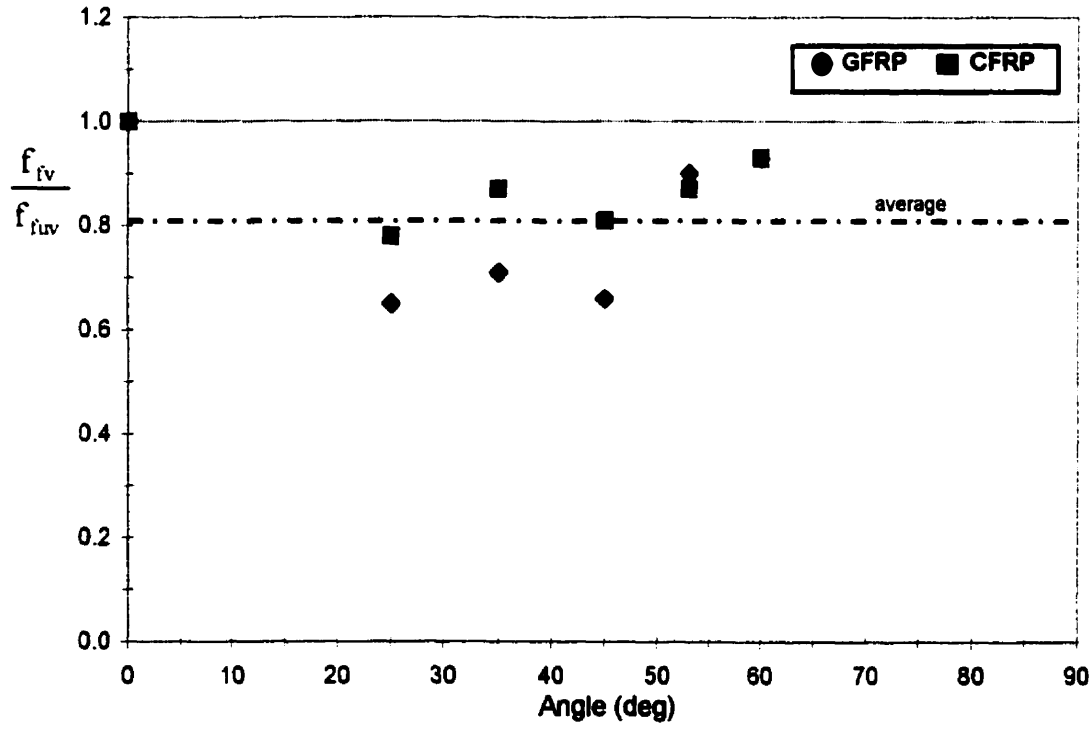

Figure 4-22 Truss model stress distribution

The predictions of the truss model correspond to the ultimate strain results mentioned previously. The measured average ultimate strain ratio of 0.83 from the tests agrees with the average stress ratio of this model of 0.810. This shows that the truss model provides an accurate and realistic prediction of the behaviour of the inclined crack specimens as compared to the bonded model. Using Figure 4-22 it can be concluded that based on the inclined crack effect, the strength in the FRP stirrups is 80 percent of the guaranteed strength in the direction of the fibres.

4.8 Related Studies

Full-scale beam tests were carried out in conjunction with this study at the University of Manitoba. FRP for shear reinforcement was investigated using 10 concrete beams reinforced with FRP as shear and longitudinal reinforcement. The parameters were the type of FRP shear reinforcement, the stirrup spacing, and the type of longitudinal reinforcement. In comparison to the individual stirrup tests, similar results were obtained. It was found that the stirrups in the beams always failed at the bend location. This indicates that between the effect of the bend and the inclined crack effect the reduced capacity at the bend location governs. Reductions of 50 percent of the capacity of the stirrups in the direction of the fibres were found as compared to 35 percent found in the current study. The higher values in the beam tests result from the group action of

the stirrups acting together instead of the isolation of the single stirrup tests. The inclined crack effect was not evident in the beam specimens due to the domination of the bend effect.

CHAPTER 5: SUMMARY AND CONCLUSIONS

The experimental program consisted of two phases designed to investigate the strength of FRP stirrups, as affected by the bend and the kinking action across inclined cracks. The first phase consisted of 101 specimens specially designed to investigate the strength reductions due to bending straight FRP bars into stirrup configuration. Based on the test results, design equations were introduced to predict the strength of the stirrups. Phase two of the program involved 12 unique specimens designed to evaluate the strength reductions due to the inclined crack effect. Based on analysis of the test results, two models are used to describe the load transfer mechanism. From the experimental program and the analysis discussed in this thesis, the following conclusions can be drawn:

1. Various FRP materials showed unique failure mechanisms

(a) The failure in the Leadline stirrups is a result of debonding between the inner fibres and the outer resin coating.

(b) Failure of the C-BAR bend specimens was initiated at points of imperfection along the bar. "Wavy" fibres caused premature failure and made it impossible to achieve the full guaranteed strength of the bar in the direction of the fibres.

2. The strength of the FRP stirrups was reduced due to the bend effect as influenced by:

- **reduction in bend radius**
- **reduction in embedment length**
- **anchorage conditions**
- **reduction in tail length**

(a) As the bend radius is decreased, the stirrup capacity is also decreased to due an increase in stress level at the bend. To achieve a stirrup capacity greater than 50 percent of the guaranteed strength in the direction of the fibres a bend radius to bar diameter ratio r_b/d_e of 4.0 for CFCC and C-BAR stirrups and 7.0 for the Leadline stirrups is recommended.

(b) By decreasing the embedment length, the strength capacity is reduced to a minimum value of 35 percent of the guaranteed capacity in the direction of the fibres.

(c) The full guaranteed strength of the stirrups in the direction of the fibres can be developed at embedment length to diameter ratios, l_d/d_e, of 20 for CFCC Type A stirrups (minimum tail length l_d* of $6d_e$), 16 for the CFCC Type B stirrups

and 42 for the Leadline stirrups. The proposed equations of Chapter 4 can be used for intermediate values of embedment length to estimate the strength.

(d) In general, the Type B (continuous) anchorage is stronger than the Type A (standard hook) anchorage unless a sufficient tail length, l_d*, is provided. By decreasing the tail length in the Type A anchorage, the stirrup capacity is reduced through slippage of the tail around the bend for CFCC stirrups but there is no significant change for the large radius Leadline specimens and the C-BAR specimens.

(e) A tail length to diameter ratio, l_d*/de, of 15 for CFCC Type A stirrups is sufficient to achieve the full guaranteed strength in the direction of the fibres. The proposed equation can be used to predict the strength at value below 15. A tail length to diameter ratio of 6 is sufficient to develop the guaranteed strength in the C-BAR specimens.

3. **The bend radius of the stirrup, r_b, to be used shall not be less than four times the effective bar diameter or 50mm, whichever is greater. The tail length, l_d^*, to be used shall not be less than six times the effective bar diameter of 70mm, whichever is greater.**

4. Using the "bonded" model to describe the load-transfer mechanism, the strength of the FRP stirrups was reduced due to the inclined crack effect as affected by:

- **Increase in crack angle**
- **Material Type**

(a) The FRP stirrup strength is reduced as the angle is increased. The strength could be as low as 65 percent of the guaranteed strength in the direction of the fibres.

(b) A new equation proposed for the inclined crack specimens conservatively predicts the capacity of an FRP stirrup with respect to the inclined crack angle.

5. The "truss" model provides a more accurate description of specimen behaviour and shows no correlation between inclined crack angle and stirrup capacity.

(a) The measured average ultimate strain ratio for all of the specimens was 0.831. The "truss" model of the load-transfer mechanism (no shear stresses in the bars) provides a stress ratio of 0.81 which corresponds to the measured

average ultimate strain ratio. The "truss" model therefore is a more accurate model for the behaviour of the specimens.

(b) The stirrup capacity for both materials was unaffected by a varying angle when stresses were provided by the "truss" model.

6. The bend effect governs the strength of FRP stirrups in concrete structures

The bend effect reduces stirrup strength capacity to 35 percent of the guaranteed strength in the direction of the fibres whereas the inclined crack effect produces a capacity as low as 65 percent of the guaranteed. Therefore in beam action the bend effect is the most critical and will govern the behaviour. However, with deep beams where the embedment length is sufficient to develop the full strength of the stirrup, the inclined crack effect could govern.

REFERENCES

1. Abdelrahman, A.A. and S.H. Rizkalla, "Advanced Composites For Concrete Structures," *Fifth International Colloquium On Concrete In Developing Countries*, Department of Civil and Geological Engineering, University of Manitoba, Winnipeg, Manitoba, January 1994.

2. ASTM C39-96, 1996; "Standard Test Method for Compressive Strength of Cylindrical Concrete Specimens," developed by ASTM subcommittee C09.61, 5 p.

3. Bank, Lawrence C., "Properties of FRP Reinforcements for Concrete", *Fiber-Reinforced-Plastic (FRP) Reinforcement for Concrete Structures: Properties and Applications*. A. Nanni (Editor), Elsevier Science Publishers B.V., 1993, pp. 59-85.

4. Clarke, J., "Alternative Materials for the Reinforcement and Prestressing of Concrete", 1st edition, Blackie Academic and Professional, Great Britain, 1993.

5. Currier, J., Fogstad, C., Walrath, D., and C. Dolan, "Bond Development of Thermoplastic FRP Shear Reinforcement Stirrups," *Proceedings of the Third Materials Engineering Conference*, ASCE, San Diego, CA, 1994, pp. 592-597.

6. Daniel, Isaac M., and Ori Ishai, "Engineering Mechanics of Composite Materials", Oxford University, New York, 1994.

7. Dolan, Charles W., "FRP Development in the United States", *Fiber-Reinforced-Plastic (FRP) Reinforcement for Concrete Structures: Properties and Applications*. A. Nanni (Editor), Elsevier Science Publishers B.V., 1993, pp. 129-155.

8. Duranovic, N., Pilakoutas, K., and P. Waldron, "Tests on Concrete Beams Reinforced with Glass Fibre Reinforced Plastic Bars," *Proceedings of the Third International Symposium on Non-Metallic (FRP) Reinforcement for Concrete Structures*, Sapporo, Japan, Oct. 1997, Vol. 2, pp. 479-486.

9. Ehsani, M.R., H. Saadatmanesh, and S. Tao, "Bond of Hooked Glass Fibre Reinforced Plastic (GFRP) Reinforcing Bars to Concrete", *ACI Materials Journal*, Vol. 92, No. 4, July-August 1995, pp. 391-400.

10. Erki, M.A. and S.H. Rizkalla. "FRP Reinforcements for Concrete Structures: A Sample of International Production". ca. 1994, p. 11

11. Hull, Derek, "An introduction to composite materials", Cambridge University Press, New York, NY, 1981.

12. Ishihara, K., Obara, T., Sato, Y., Ueda, T., and Y. Kakuta, "Evaluation of Ultimate Strength of FRP Rods at Bent-Up Portion," *Proceedings of the Third International Symposium on Non-Metallic (FRP) Reinforcement for Concrete Structures*, Sapporo, Japan, Oct. 1997, Vol 2, pp. 27-34.

13. Japanese Society of Civil Engineers, JSCE, "Recommendations for Design and Construction of Concrete Structures using Continuous Fibre Reinforcing Materials," *Concrete Engineering Series 23*, A. Machida (ed.), 1997.

14. Kanematsu, H., Sato, Y., Ueda, T., and Kakuta, Y., "A Study on Failure Criteria of FRP Rods Subject to Tensile and Shear Force," *Proceedings, FIP Symposium '93*, Kyoto, Japan, Oct. 1993, pp. 743-750.

15. Kawata, Kozo, and Takashi Akasaka (eds.), "Composite Materials; Mechanics, Mechanical Properties and Fabrication", Applied Science Publishers, Englewood, NJ, 1982.

16. Mallick, P.K., "Fiber-Reinforced Composites: Manufacturing, and Design", 2nd edition, Marcel Dekker, Inc., New York, 1993.

17. Marshal Industries Composites, "C-BAR Composite Reinforcing Rods: The Future of Concrete Reinforcement", *Product Manual*, USA, 1997.

18. Maruyama, T., M. Honma, and H. Okamura, "Experimental Study on the Diagonal Tensile Characteristics of Various Fiber Reinforced Plastic Rods" *Transactions of the Japan Concrete Institute*, Vol. 11, 1989, pp. 193-198.

19. Maruyama, T., Honma, M., and Okamura, H., "Experimental Study on Tensile Strength of Bent Portion of FRP Rods," *ACI SP-138*, American Concrete Institute, Farmington Hills, 1993, pp. 163-176.

20. Minor, John and James O. Jirsa, "Behaviour of Bent Bar Anchorages", *ACI Journal*, April 1975, pp. 141-149.

21. Mitsubishi Chemical Corporation, "Leadline Carbon Fiber Tendons/Bars", *Product Manual*, Japan, 1992.

22. Miyata, S., Tottori, S., Terada, T., and Sekijima, K., "Experimental Study on Tensile Strength of FRP Bent Bar," *Transactions of the Japan Concrete Institute*, Vol. 11, 1989, pp.185-192.

23. Mochizuki, S., Y. Matsuzaki, and M. Sugita, "Evaluation Items and Methods of FRP Reinforcement as Structural Elements", *Transactions of the Japan Concrete Institute* Vol. 11, 1989. pp. 117-131.

24. Mufti, A.A., M-A. Erki and L.G. Jaeger, "Advanced Composite Materials with Applications to Bridges", *The Canadian Society for Civil Engineering*, Montreal, May 1991, p. 22.

25. Nagasaka, T., Fukuyama, H., Tanigaki, M., "Shear Performance of Concrete Beams Reinforced with FRP Stirrups", *Transactions of the Japan Concrete Institute*, Vol. 11, 1989, pp. 789-811.

26. Nakamura, H., and Higai, T., "Evaluation of Shear Strength of Concrete Beams Reinforced with FRP," *Concrete Library International*, Proceedings of Japan Society of Civil Engineers, No. 26, December 1995, pp. 111-123.

27. Rizkalla, S.H., et al., "Material Properties of C-BAR™ Reinforcing Rods", *Research report submitted to Reichold Chemicals Inc.*, 1997.

28. Souroushian, P., et al, "Pullout Behaviour of Hooked Bars in Exterior Beam-Column Connections", *ACI Structural Journal*, May-June 1988, pp. 269-276.

29. Tokyo Rope Manufacturing Company, Ltd., "Technical Data on Carbon Fiber Composite Cables (CFCC)", *Product Manual*, Japan, 1993.

30. Ueda, T., Sato, Y., Kakuta, Y., Imamura, A., and Kanematsu, H., "Failure Criteria for FRP Rods Subjected to a Combination of Tensile and Shear Forces," *Proceedings of the Second International RILEM Symposium (FRPRCS-2), Non-Metallic (FRP) Reinforcement for Concrete Structures*, Ghent, Belgium, Aug. 1995, pp. 26-33.